UNIVERSITA' DEGLI STUDI DI NAPOLI "FEDERICO II"

FACOLTA' DI FARMACIA

Dipartimento di Farmacologia Sperimentale

TESI DI DOTTORATO DI RICERCA IN SCIENZA DEL FARMACO

XXI CICLO

IRON METABOLISM IN AN *IN VITRO* MODEL OF CARDIAC ISCHEMIA : HYPOXIC INJURY AND PROTECTIVE STRATEGIES

TUTORE
Chiar.mo Prof. R. Santamaria

COORDINATORE
Chiar.mo Prof.M.Valeria D'Auria

DOTTORANDA

Dott. Virginia Cozzolino

2005-2008

ACKNOWLEDGMENTS

I would like to thank many of the special people who assisted me through the completion of the thesis.

First, my sincere gratitude goes to my supervisor Prof. Rita Santamaria for her guidance, encouragement and great support through the past three years. I am also thankful to Prof. Alfredo Colonna for his constant assistance, for financial support and for his precious suggestions. Their invaluable advices and constant supervisions were indispensable for my research work and my scientific formation.

Gratitude also goes to Prof. Alfredo Colonna, chief of the Department of Experimental Pharmacology, and to Prof. Maria Valeria D'Auria, director of my PhD.

I wish to express my gratitude to Dr. Carlo Irace for his assistance and friendship in the laboratory and to all colleagues for their continuous support.

This Doctorate thesis is dedicated to my family, to my bestfriend Maria Gabriella Dattolo and to Paolo Battiloro a very important person. Thanks for you care, love, encouragement and confidence in me for all these years.

TABLE OF CONTENTS

Aim of research

Material and Methods

Results

LIST OF FIGURES

LIST OF TABLES

INTRODUCTION

1. The importance of iron

1.1 Iron : an indispensable and potentially toxic nutrient

Iron is a basic requirement for most forms of life, including humans and most bacterial species and is one of the most commonly used metals in biological system. In fact, in vertebrates several physiological processes, as well as oxygen transport, cellular respiration, DNA synthesis, production of various neurotransmitters and hormones, xenobiotics metabolism and some aspects of host defense make use of iron-containing proteins.

Iron is one of the most important trace elements required and the adequate daily supply is in the low milligram range (Wood ***et al***., 2006). The total iron content of body varies with age, sex, nutrition and state of health. Normal adult man is

estimated to contain 4.5 g of iron, of which about 60-70% as haemoglobin and 3% as myoglobin.

The critical role of iron in human health is supported by the relationship between sufficient iron intake and the prevention of some diseases (Neilands, 1991). In fact iron deficiency causes anemia, impairs muscle, immune and cognitive functions and can increase the incidence of low birthweight and preterm delivery. At present, the nutritional importance of iron is evident, given the worldwide prevalence of disorders arising from iron deficiency and the evidence of the central role of iron-containing proteins in multiple cellular processes (Bothwell, 1995). However, when present at levels that exceed the capacity of organism to safely use it, iron can be toxic because of its ability to promote oxidation of lipids, proteins and other cellular components. High levels of iron have been associated with increased incidence of some cancers, dysfunction of organs, such as heart, pancreas, or liver and development of neurodegenerative disorders (Halliwell, 1992).

1.2 Toxicity of iron

The ability of Fe(II) to donate electrons and of Fe(III) to accept electrons is a fundamental feature for many biochemical reactions. However iron can also be potentially toxic because under aerobic conditions it can catalyze the production of reactive oxygen species (ROS) that can cause damage to a wide variety of cellular structures and ultimately kill the cell (Aisen ***et al***.,1990). Iron's toxicity

is largely based on Fenton and Haber-Weiss chemistry (Fig. 1A), where catalytic amounts of iron are sufficient to yield hydroxyl radicals ($OH^{\cdot}$) from superoxide ($O_2^{\cdot-}$) and hydrogen peroxide (H_2O_2), collectively known as "reactive oxygen intermediates" (ROIs) (Halliwell and Gutteridge, 1990). ROIs are byproducts of the aerobic respiration and arise by incomplete reduction of oxygen in mitochondria. Iron catalyzes the generation also of organic reactive species, such as peroxyl ($ROO^{\cdot}$), alkoxyl ($RO^{\cdot}$), thiyl ($RS^{\cdot}$), or thiyl-peroxyl ($RSOO^{\cdot}$) radicals (Fig. 1B).

A.

$Fe(II) + H_2O_2 \rightarrow Fe(III) + OH^- + OH^{\cdot}$ (Fenton)

$Fe(III) + O_2^{\cdot-} \rightarrow Fe(II) + O_2$

Net reaction:

$H_2O_2 + O_2^{\cdot-} \xrightarrow{Fe} OH^- + OH^{\cdot} + O_2$ (Haber-Weiss)

B.

$Fe(II) + ROOH \rightarrow Fe(III) + OH^{\cdot} + RO^{\cdot}$

$Fe(III) + ROOH \rightarrow Fe(II) + H^+ + ROO^{\cdot}$

$RSH + OH^{\cdot} \rightarrow RS^{\cdot} + H_2O$

$RS^{\cdot} + O_2 \rightarrow ROO^{\cdot}$

C.

Heme-Fe(II)-O_2 + H_2O_2 $\rightarrow$ Heme-Fe(IV)-$OH^{\cdot}$ + O_2 + $OH^{\cdot}$

Heme-Fe(IV)-$OH^{\cdot}$ + ROOH $\rightarrow$ Heme-Fe(III) + $ROO^{\cdot}$ + H_2O_2

D.

$$Fe\ (II) + H_2O_2 \rightarrow Fe\ (II)\text{-}O + H_2O$$

$$Fe\ (II) + O_2 \rightarrow [Fe\ (II)\text{-}O_2 \rightarrow Fe\ (III)\text{-}\ O_2^{\cdot-}] \rightarrow Fe\ (III) + O_2^{\cdot-}$$

Fig. 1. Iron and free radicals
(A) Iron-catalyzed generation of the hydroxyl radical via the Fenton reaction; the net Haber-Weiss reaction is also indicated. (B) Iron-catalyzed generation of organic radicals. (C) Heme-catalyzed production of oxygen radicals via oxoferryl intermediates. (D) Direct interaction of iron with oxygen.

Interestingly, heme iron may catalyze the formation of radicals, mainly via formation of oxoferryl intermediates (Ryter and Tyrrell, 2000) (Fig. 1C). Finally, ferrous iron can contribute as reactant, rather than as catalyst, to free radical generation by a direct interaction with oxygen, via ferryl (Fe^{2+}-O) or perferryl (Fe^{2+}-O_2) iron intermediates.

An increase in the levels of reactive oxygen species beyond the antioxidant capacity of the cell causes oxidative stress and occurs in many pathological conditions, such as chronic inflammation, ischemia-reperfusion injury or neurodegeneration (Ischiropoulos and Beckman, 2003). Excess of redox active iron exacerbates oxidative stress and leads to tissue degeneration.

Under physiological conditions, extracellular iron is bound to transferrin, a glycoprotein working as the plasma iron transporter, which maintains iron soluble and non-toxic (Ponka *et al.,*1998). In healthy individuals, only 30% of

circulating transferrin binds to iron. In pathological iron overload conditions, iron gradually saturates the iron-binding capacity of transferrin and forms redox-active, low-molecular-weight chelates. Non-transferrin-bound iron ultimately gets into tissues resulting in tissue injury.

1.3 Cellular iron uptake

Transferrin receptor provides for entrance of transferrin to cells. Two types of receptor have been described. The first and more studied of these is known as transferrin receptor 1 (TfR1). It consists of two disulfide-bonded identical 90 KDa subunits, each bearing three asparagines-linked and one threonine-linked carbohydrate chains. TfR1 is expressed by all iron-requiring cells, and is more abundant than transferrin receptor 2 (TfR2). The first 61 amino acids of each subunit form the cytoplasmatic domain, and a membrane-anchoring hydrophobic sequence of residues 62-89 that spans the lipid bilayer once. The rest of the protein, bearing the transferrin recognition sites, lies in the external region. The TfR2 exists in two forms, TfR2-α, with a 45% sequence identity to TfR1 and TfR2-β, lacking of the N-terminal portion, including the cytoplasmic and transmembrane regions. Expression of TfR2 is predominantly in liver and in some proliferating cells (Brissot ***et al.***, 2004).

Transferrin (Tf) binds to the TfR at the cell surface and is internalized though clathrin-coated pits into endosomes via a well characterized pathway (fig. 2). At the acidic pH of the endosome, iron dissociates from Tf and goes into the cytoplasm, presumably via a membrane transporter. The rate of iron release from Tf to cells depends on the pH of the endosome and its association with the TfR (Sipe *et al.,* 1991), but the efficiency is probably less than 100%. Endosomal pH varies with cell type, ranging from 6 to 5.5.

Even the lowest pH achieved by endosomes, however, is not sufficient to remove iron from transferrin in the few minutes, so that other mechanisms must participate in iron release. Such mechanisms might include the availability of iron-sequestering molecules, such as citrate or ATP, or the reduction of iron in the transferrin-transferrin receptor complex, as suggested by identification of a membrane ferrireductase (McKie *et al*., 2001). After the return of the receptor/Tf complex to the cell surface, the extracellular pH triggers the release of apo-Tf, allowing another round of binding and endocytosis to begin.

The transferrin/TfR1 pathway represents the major way for cellular iron uptake and some cell types (for example erytroid cells) depend on it for iron acquisition.

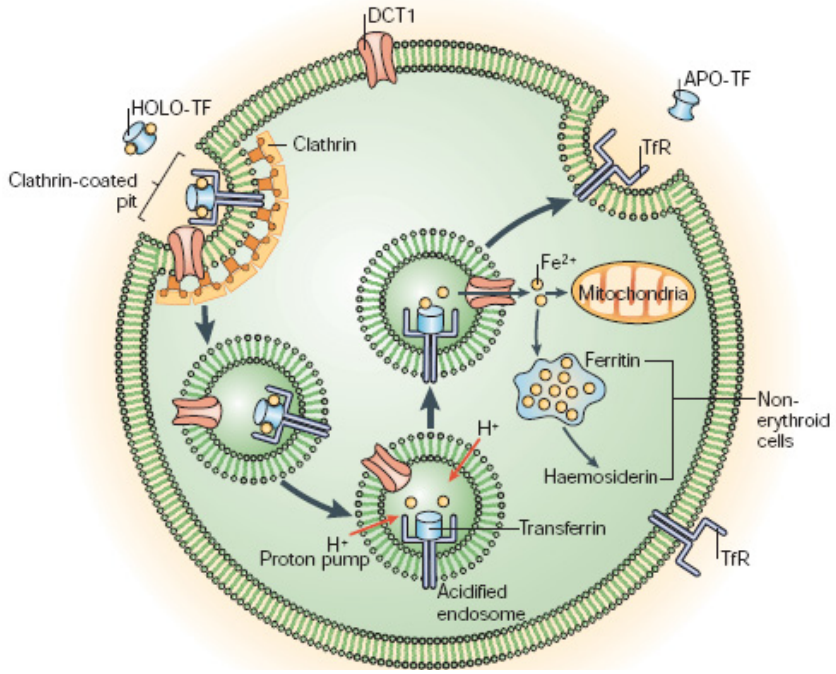

Fig. 2. The transferrin cycle
Transferrin binds to the transferrin receptor (TfR) at the cell surface in proximity of clathrin-coated pits, which invaginate to initiate endocytosis and form specialized endosomes. At acid pH iron is released from transferrin (Tf) and is transported out of the endosomes by the divalent cation transporter DCT1 or DMT1. Apotransferrin come again to the cell membrane to participate in further rounds of iron delivery.

1.4 Absorption of iron

The absorption of dietary iron takes place in the duodenum and small intestine. From total iron intake only 5-15% is absorbed. Absorption depends on many factors, as requirement of the organism and type of iron (ferric or ferrous form). Before the entrance into enterocytes, insoluble ferric ion can be reduced

by a cytochrome b-like hemoprotein Dcytb at the plasma membrane level (Fig. 3) (McKie ***et al.*****,** 2001). A transmembrane protein Nramp2 (also known as DCT1 or DMT1) is expressed on the lumen of the intestine and transports ferrous ion across the membrane. DMT1 is a proton/divalent metal co-transporter that carries several transition metals including iron, manganese and cobalt (Gunshin ***et al.***, 1997). The DMT1 mRNA contains IREs and the expression of the protein is regulated post-transcriptionally by the iron level.

DMT1 is also involved in the transport of ferrous ion across endosomal membrane into the cytoplasm after the transferrin-iron release from transferrin in endosomes. After the absorption of iron by intestinal Nramp2, the transport of iron across the basolateral membrane to the portal vein occurs. The iron-regulated transporter-1 specifically expressed in the duodenal mucosa, IREG1, also known as ferroportin 1, functions in the stimulation of iron efflux from the cells. Ferroportin 1 is a transmembrane protein that transports iron from the inside of a cell to the outside of it. It is located on the surface of cells that store or transport iron, as enterocytes, hepatocytes and macrophages. The expression of this protein is dependent on the iron absorption and the 5´-UTR region of its mRNA contains a functional iron-responsive element (IRE) (Donovan ***et al.***, 2000).

In addition, for the export of iron from non-intestinal cells the ceruloplasmin is required. This protein oxidizes ferrous ion exported by ferroportin 1 to ferric ion to facilitate the binding of iron to transferrin. Humans and mice deficient in

ceruloplasmin accumulate iron in several cells, including macrophages, neural cells and hepatocytes, indicating that a serum ferroxidase activity is essential for the mobilization of iron between macrophages and other tissues.

Another protein implicated in iron transport is the hephaestin, a transmembrane copper-dependent ferroxidase responsible for transporting dietary iron from intestinal enterocytes into the circulatory system (Anderson 1998; Vulpe ***et al***., 1999). Finally, a central role to maintain iron homeostasisis is carried out by hepcidin, a peptide hormone produced by the liver. In fact, this protein inhibits ferroportin 1, the cellular iron exporter, reducing iron absorption. Thus, hepcidin appears to be the master negative regulator of systemic iron homeostasis in humans and other mammals (Ganz 2003; Nemeth ***et al.***, 2004).

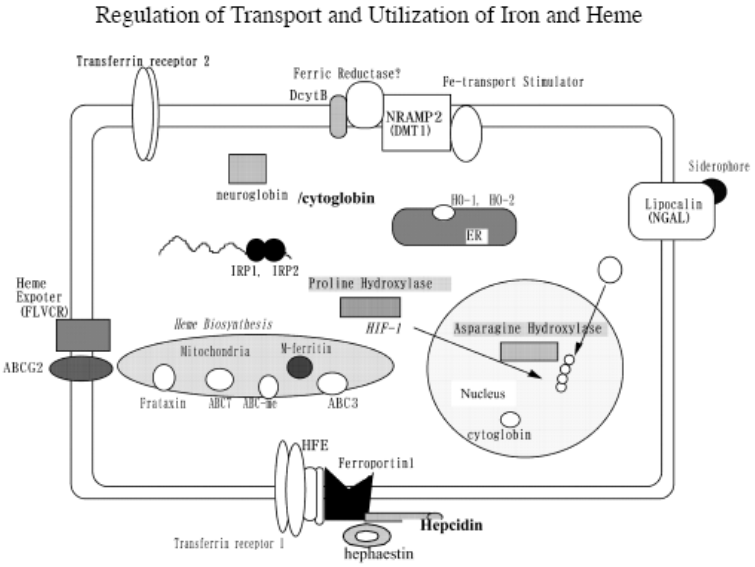

Fig. 3. Proteins involved in the transport and utilization of iron and heme

HFE, DcytB, hephaestin, transferrin receptor 2, ferroportin 1, and hepcidin are involved in iron metabolism; HIF-1α proline hydroxylase and HIF-1α asparagine hydroxylase are regulators as an oxygen sensor.

1.5 Cellular iron utilization

After the entry into the cytosol iron is distributed to the various intracellular proteins and organelles that need iron. Generally, there are three possible fates for iron in the cytoplasm: a) synthesis of iron-containing proteins; b) storage; c) export out of the cell. The use of intracellular iron in metabolic pathways or into storage proteins depends on the cellular iron condition and metabolic requirements of the cell. In mitochondria iron is involved in assemblage of heme and FeS proteins and in liver and in erythroid cells a large fraction of iron is incorporated into protoporphyrin IX to heme formation (Ponka *et al*., 1997).

As concern the mitochondrial iron trafficking various components of mitochondrial iron uptake and efflux pathway have identified (Allikmets *et al*., 1999; Lange *et al*., 1999) and several data indicate that mitochondria have a dynamic iron pool that functionally interacts with the cytosolic iron pool (Knight *et al*., 1998).

A critical aspect of the maintenance of cellular iron homeostasis is the control of the expression of genes encoding proteins required for the uptake (TfR1, DMT1), storage (ferritin) or export (FPN) of iron (McKie *et al*., 2000; Abbound *et al*., 2000). To coordinate these processes, sensing of cellular iron status is required. Iron regulatory proteins (IRPs) are central components of a sensory and regulatory system required for the maintenance of iron homeostasis in vertebrates.

1.6 Ferritin structure and function

Ferritin is a ubiquitous and highly conserved iron-binding protein. In vertebrates, the cytosolic form consists of two subunits, termed H and L. Twenty-four ferritin subunits assemble to form the apoferritin shell (fig. 4). Each apoferritin molecule of 450 KDa can sequester up to approximately 4500 iron atoms (Harrison *et al*., 1996). Depending on the tissue type and physiologic status of the cell, ratio of H to L subunits in ferritin can vary widely, from predominantly L in such tissues as liver and spleen, to predominantly H in heart and kidney. The H to L ratio is readily modified in many inflammatory and infectious conditions, and in response to xenobiotic stress, differentiation and developmental processes, as well as other stimuli. Ferritin H and L subunits are encoded by different genes. Although a single functional H and L gene was thought to be expressed in all vertebrate species, a

functional mitochondrial ferritin gene has been described (Levi *et al*., 2001). Multiple pseudogenes are also present.

Moreover ferritin has enzymatic properties, converting Fe (II) to Fe (III) when iron is internalized and sequestered in the ferritin mineral core. This function is evolutionarily conserved and it is an intrinsic characteristic of the H subunit, which has a ferroxidase activity (Rucker *et al*., 1996).

Small quantities of ferritin are present in human serum and are elevated in conditions of iron overload and inflammation (Torti *et al*., 1994). Serum ferritin is iron-poor and immunologically resembles ferritin L.

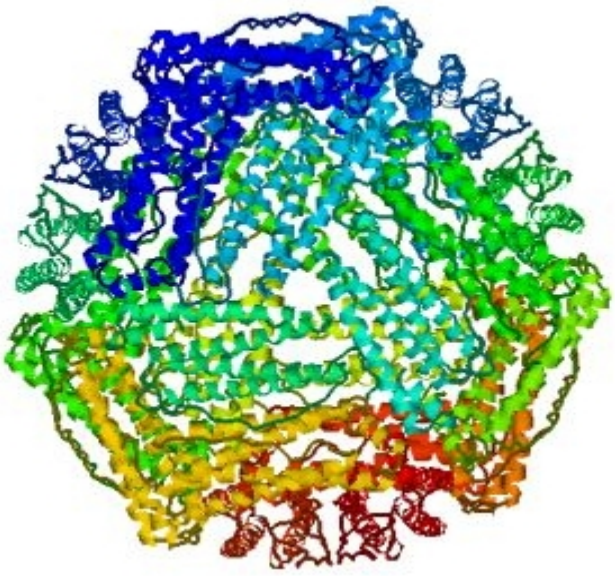

Fig. 4. Ferritin structure
Twenty-four ferritin subunits assemble to form the apoferritin shell, that has a molecular weight of ~ 450 KDa.

Despite general use of serum ferritin as clinical indicator of body iron stores, little is known of source of this ferritin.

The critical role of ferritin in cellular iron homeostasis is closely linked to its function of iron sequestration. The toxicity of iron in cellular systems is attributable in large part to its capacity to participate in the generation of reactive species, which can directly damage DNA, lipids, and proteins, leading to cellular damage. In the organism iron balance is maintained with fine regulation. Ferritin, by capturing the intracellular labile pool (Kakhlon *et al*., 2001) plays a key role in maintaining iron homeostasis. It is not surprising that H ferritin gene deletion in mice knockout is lethal (Ferreira ***et al***., 2000). Actually, is evident that regulatory factors, in addition to those that control iron flux, have an important impact on cellular ferritin. In fact, ferritin can be viewed not only as part of a group of iron metabolism regulatory proteins that include transferrin and transferrin receptor, but also as a member of protein family that orchestrates the cellular defense against stress and inflammation.

2. Regulation of ferritin and transferrin receptor expression

2.1 Post-trascriptional regulation by iron regulatory proteins

The cellular levels of ferritin and transferrin receptor (TfR) are primarily regulated at translational level by changes in iron availability, through interactions between iron regulatory proteins (IRP1 and IRP2) and iron-responsive elements (IRE) contained within the 5' UTR of H- and L-ferritin mRNA and the 3' UTR of TfRmRNA (fig. 5). When cellular iron levels are low, IRPs binds to the IRE cis-element in ferritin mRNA and protein translation is blocked. When intracellular iron levels rise, IRP1 is no longer able to bind IRE, IRP2 is degraded and ferritin mRNA is efficiently translated. When cellular iron levels are low, IRPs binds to the IRE cis-element in ferritin mRNA and protein translation is blocked. When intracellular iron levels rise, IRP1 is no longer able to bind IRE, IRP2 is degraded and ferritin mRNA is efficiently translated. On the contrary, the TfR expression is largely controlled through changes in RNA degradation (Wallander ***et al***., 2006). During low iron conditions, IRPs bind to 3' UTR IREs in Tf R mRNA, resulting in the stabilization of the TfR mRNA. During high iron conditions, IRPs lose their affinity for IREs mediating degradation of the Tf R mRNA.

There are two RNA binding proteins, iron regulatory proteins 1 and 2 (IRP1 and IRP2), that bind to IRE stem loop. These proteins are regulated differently:

IRP1 is an iron-sulfur cluster protein that exists in two forms. When iron level is high , it exist as a cytosolic aconitase. When iron islow, it assumes an open configuration associated with the loss of iron atoms in the iron-sulfur cluster, and can bind the IRE stem loop. In contrast, IRP2 is regulated by its degradation: IRP2 protein is abundant in iron deficiency, but is degraded rapidly in iron overload (Iwai ***et al.*****,** 1998).

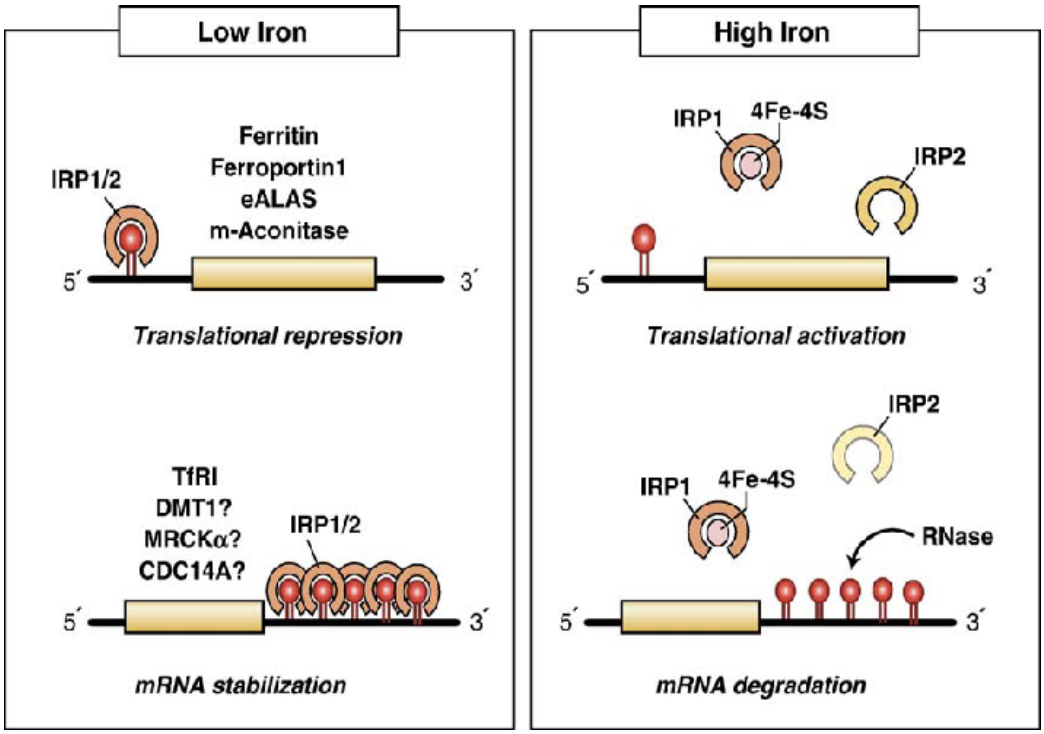

Fig. 5. Cellular regulation of mammalian iron homeostasis by the IRPs. Decreased iron supply activates binding of IRPs to IRE resulting in translational inhibition of the mRNAs encoding ferritin and stabilization of the

Tf R mRNA. During high iron conditions, IRPs lose their affinity for IREs, increasing translation of ferritin mRNAs and degradation of the Tf R mRNA.

2.2 IRP1 and IRP2

IRP1, an evolutionarily conserved protein, is highly homologous with mitochondrial (m-)aconitase, which converts citrate into isocitrate in the tricarboxylic acid cycle. The informations concerning the structure of m-aconitase has allowed the construction of an model that implies a post-translational switch between an apoprotein form capable of binding iron-responsive-element (IRE) and an enzymically active protein with 4Fe-4S cluster (Eisenstein *et al.*, 1998; Wallander *et al.,* 2006*).* In the holoprotein, the four domains are in closed conformation and permit the assembly of a 4Fe-4S cubane cluster co-ordinated by cysteine residues. By contrast, as result of cluster disassembly, the apoprotein can accommodate the RNA in a cleft between domains 1-3 and 4. The switch between these two mutually exclusive functions of IRP1 is regulated by intracellular iron levels, because a high degree of aconitase activity is present under conditions of iron overload and full IRE-binding capacity exists in iron-depleted cells. The mechanism

underlying the insertion and removal of cluster, and hence the conversion between the two functions of IRP1, remain poorly defined.

IRP2 is usually less abundant and can be electrophoretically distinguished from IRP1 only in murine cell extracts. IRP2 is highly homologous with IRP1, but has two major differences: the presence of a 73-amino-acid insertion in the N-terminus and lack of aconitase activity (Cairo *et al*., 2000).

The IRP2 specific sequence mediates the characteristic way by which this protein is regulated: in presence of high iron levels, IRP2 is rapidly targeted to proteasome-mediated degradation (Iwai *et al.*, 1998) (fig. 6).

Although both IRP1 and IRP2 bind the IRE and exert the same effect on ferritin and TfR synthesis, these proteins may have distinct tissue-specific role. The ratios of IRP1/IRP2 differ in a tissue-specific fashion, with IRP1 being more abundant than IRP2 in liver, kidney, intestine, and brain, and less abundant in pituitary and pro-B-lymphocytic cell line (Eisenstein, 2000).

A e B

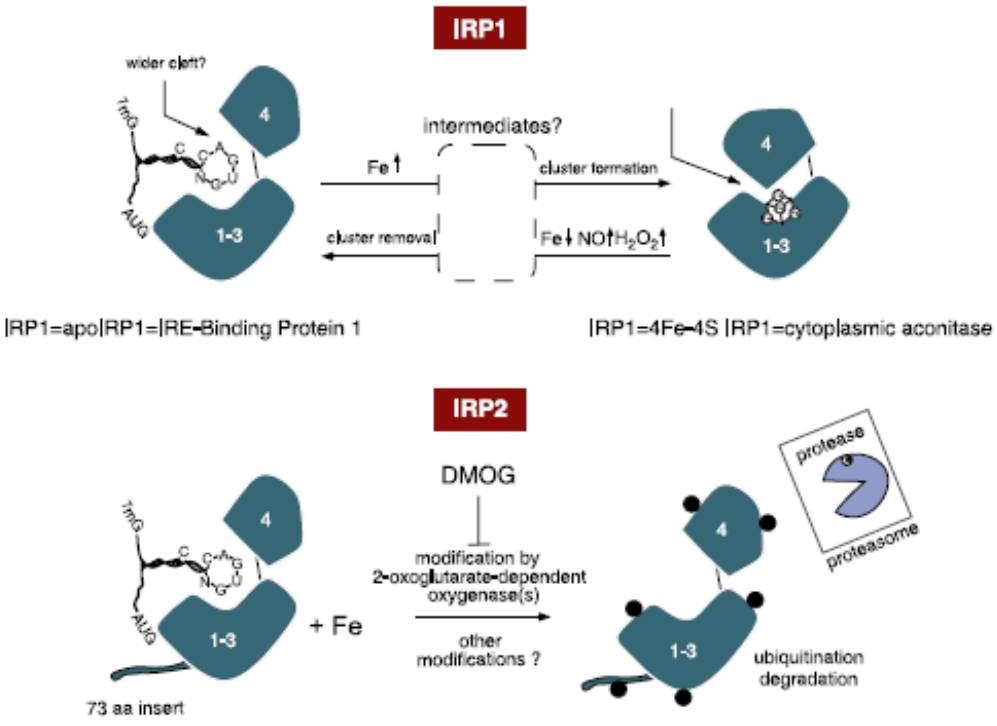

Fig. 6. **IRPs regulation by iron and other stimuli**
A) Regulation of bifunctional IRP1 protein in response to iron and other stimuli *via* iron-sulfur cluster switch.
B) Iron-dependent degradation of IRP2.

Moreover, IRP2 deletion in knockout mice determines a pronounced misregulation of iron metabolism in the intestinal mucosa and central nervous system (LaVaute *et al*., 2001).

2.3 IRPs regulation by other stimuli

IRPs are considered as intracellular iron sensors, but they also respond to other stimuli. Exposure of cells to hydrogen peroxide (H_2O_2) or nitric oxide (NO) induces IRE-binding activity (Cairo *et al*., 2002) (fig. 6). The response of IRP1 to H_2O_2 and NO are complex. The H_2O_2-mediated conversion of IRP1 from cytosolic aconitase to IRE-binding protein is a result of signalling pathway rather than of direct chemical modification of the 4Fe-4S cluster by H_2O_2. The mechanism for IRP1 activation by NO is distinct. Exposure of purified IRP1 to

NO *in vitro* was shown to activate IRE binding (Soum *et al*., 2003), although this effect was only partial.

The IRPs RNA-binding activity is also regulated by protein phosphorylation, hypoxia conditions, as well as by oxalomalic acid, a known inhibitor of aconitase/IRP1 (Wallander ***et al***., 2006; Festa ***et al***., 2000).

3. Hypoxia

Hypoxia is oxygen starving at the tissue and cellular levels. It is caused by reduction of oxygen supply in blood and in tissues below physiological levels. Severe hypoxia can result in anoxia, a complete loss of oxygen to an area of tissue.

There are four major types of hypoxia. The first type, hypoxic hypoxia, is decrease of fraction of inhaled oxygen possibly due to hyperventilation from respiratory depression or altitude above sea level. The second type of hypoxia is termed anaemic hypoxia, and is characterized by a decrease in the amount of haemoglobin that binds oxygen in the blood. This can be caused by multiple factors, including but not limited to: blood loss, reduced red blood cell production, carbon monoxide poisoning, and a genetic defect of haemoglobin. Stagnant hypoxia, the third type of hypoxia that has been defined, results in low blood flow and is caused by vasoconstriction and/or heart failure. The

fourth type of hypoxia is hystotoxic hypoxia, a poisoning of oxidative enzymes that causes vasodilatation in brain arteries and veins, resulting in more blood flow to the brain tissues. This response is probably mediated by nitric oxide (NO) and adenosine.

Hypoxia is a fundamental angiogenic stimulus and an important mediator of this primary stimulus is the transcription factor hypoxia-inducible factor-1 (HIF-1α) (Semenza *et al*, 1997). The regulation of most proteins necessary for hypoxic adaptation occurs at DNA level and involves transcriptional induction *via* the binding of the transcription factor HIF-1α to the conserved sequence, 5-(A/T)CGTG-3, in the hypoxia response element (HRE) on the regulated genes. To date, more than 100 hypoxia-inducible genes have been found to be directly regulated by HIF-1.

HIF-1 is a heterodimer composed of 120 kDa HIF-1α subunit and a 91-94 kDa HIF-1α subunit. In addition to the ubiquitous HIF-1α, the HIF-1α family contains two other members, HIF-2α (Tian *et al*., 1997; Hogenesch *et al*., 1997; Ema *et al*., 1997) and HIF-3α (Gu *et al*., 1998), both of which have more restricted tissue expression (Wenger *et al*., 2002). HIF-2α and HIF-3α contain domains similar to those in HIF-1α and exhibit similar biochemical properties, such as heterodimerization with HIF-1α and DNA binding to the same DNA sequence *in vitro*. HIF-2α is also tightly regulated by oxygen tension and its complex with HIF-1α appears to be directly involved in hypoxic gene regulation, as is HIF-1α (Wiesener *et al*., 1998). However, although HIF-

3α is homologous to HIF-1α, it might be a negative regulator of hypoxia-inducible gene expression (Hara *et al*., 2001).

3.1 Regulation of HIF-1α

Under normoxic conditions HIF-1α protein undergoes prolyl hydroxylation by specific cellular prolyl hydroxylases. Hydroxylated HIF interacts with the VHL, a critical member of an E3 ubiquitin-protein ligase complex that polyubiquitylates HIF (Fig.7). Polyubiquitylation targets HIF-1α for destruction by the 26S proteosome. Under hypoxia hydroxylation does not occur and HIF-1α is stabilized and then dimerizes with HIF-1α. The heterodimeric HIFs upregulate numerous hypoxia-inducible genes, triggering physiologic responses to hypoxia..

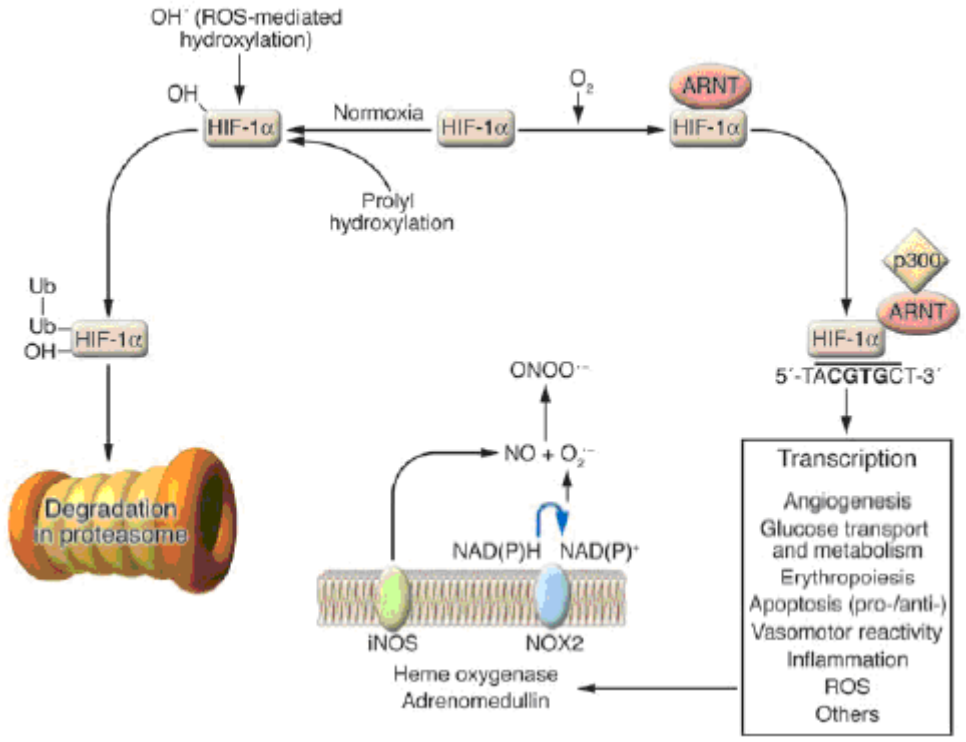

Fig.7. Transcriptional gene regulation by the hypoxiainducible factor HIF-1α. HIF-1α protein undergoes prolyl hydroxylation under normoxic conditions by specific proyl hydroxylases. Hydroxylated HIF is then degraded by the proteosome. Under hypoxia hydroxylation does not occur and HIF-1α is stabilized. The heterodimerization with ARNT forms the active HIF complex that binds to hypoxia response element in various genes.

In addition to mediating adaptation to hypoxia, HIF-1 also contributes to other cellular processes that occur under normoxic conditions, such as the development of normal tissues or tumors, the determination of cell death or survival, immune responses and the adaption to mechanical stress. Under normoxic conditions HIF-1 can be activated by various cytokines, growth

factors, transition metals, iron chelation, as well as nitric oxide (NO) (Bemis *et al*., 2004).

3.2 Hypoxia-mediated iron metabolism regulation

The genes coding for the main proteins involved in the iron metabolism respond to hypoxia. Hypoxia determines an increase in TfR RNA, despite a decrease of IRP1 activity. This increase results from hypoxia-induced stabilization of HIF-1 and increased TfR gene transcription (Tacchini *et al*., 1999). Moreover hypoxia increases transferrin gene expression in hepatoma cells (Rolfs *et al*., 1997); transferrin is a member of the HIF-1-regulated gene family. Finally, the activity of the RNA-binding proteins, IRP1 and IRP2 are regulated by hypoxia. Hypoxia exposure decreases IRP1-RNA binding activity and increases IRP2-RNA binding activity. The hypoxic increase in IRP2-RNA binding results from increased IRP2 protein levels. Recent evidence demonstrates that the response of IRP1 to hypoxia and reoxygenation can vary in a cell type specific manner (Irace *et al*., 2005).

3.3 How would hypoxia regulate iron metabolism?

One proposed mechanism of hypoxic regulation of iron metabolism is *via* hydrogen peroxide (H_2O_2), possibly from a heme-containing oxygen sensor that acts as an IRP2 degradation signal (Hanson *et al*., 1999). The use of oxygen-derived free radicals in the regulation responses appears to be a general mechanism for regulating the stability of proteins that mediate hypoxic adaptation. The hypoxia-induced changes in the level of this reactive oxygen species may involve HIF-1α activation (Fig.8).

In normoxic cells HIF-1α is rapidly degradated by a proteosomal mechanism. It has been reported that hypoxia upregulates tumor suppressor protein pVHL and this protein could be required for oxygen-dependent HIF-1α degradation. The ability of pVHL to degrade HIF1 appears to be iron-dependent. Treatment with iron chelators prevented the association of pVHL with HIF1, suggesting that iron may be necessary for the interaction of pVHL with HIF1 (Maxwell *et al*., 1999).

A close relationship exists between oxygen and iron. In fact, iron and oxygen regulate overlapping cellular activities. Both iron depletion and hypoxia compromise cellular ATP production by oxidative phosphorylation. In the iron-depleted cell, oxidative phosphorylation is arrested because this process depends on various iron-containing proteins. In hypoxic cell oxidative

phosphorylation is arrested due to oxygen deficiency. It appears that the common cellular responses to iron depletion and oxygen depletion may be cellular adaptations to compensate the ATP deprivation. In iron depletion, the cell compensates in two ways. First, to restore the free iron available for essential cellular processes, the cell tries to increase its iron uptake and decrease its iron storage. Second, while the intracellular iron is being replenished, the cell tries to find other means of generating ATP. To this aim, iron-depleted cells up-regulate glycolitic enzymes and glucose transporters *via* a HIF1α -dependent pathway. Similarly, during hypoxia the cell compensates for ATP-depletion by increasing glycolysis. The hypoxic injury causes the stabilization of HIF-1α, resulting in transcriptional up-regulation of glycolitic enzymes and glucose transporters. The restored ATP production may be an important mechanism by which iron chelators could prevent cellular injury during ischemic insult.

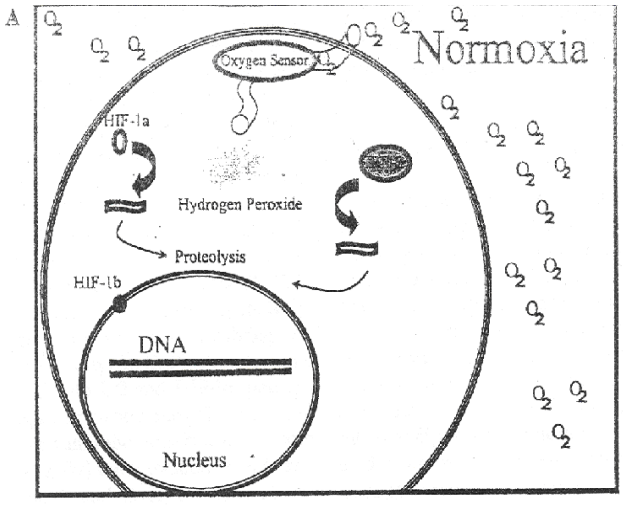

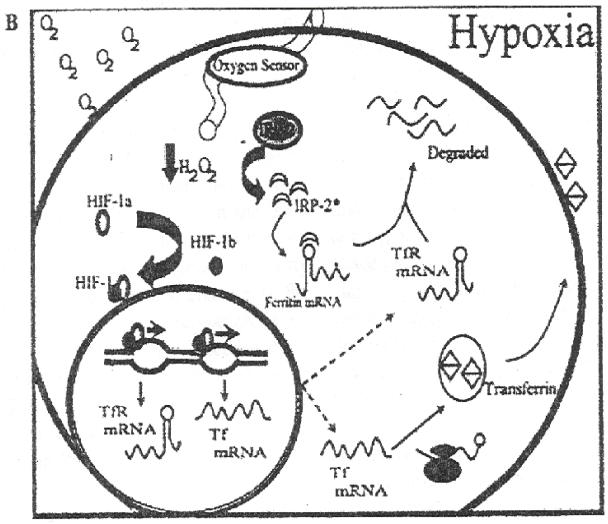

Fig. 8. Hypoxia and iron metabolism
A. Normoxic Cell. This cell is well oxygenated, and the oxygen sensor is saturated. This may lead to generation of H_2O_2, which facilitate the degradation of HIF-1α and IRP-2.
B. Hypoxic Cell. HIF-1α is stabilized and after heterodimerizing with HIF-1β, translocates into the nucleus, where it binds to the hypoxia response element (HRE) upstream of a multitude of genes, including TfR and Tf. IRP2 is also stabilized and activated.

4. Myocardial ischemia

Myocardial ischemia occurs when the heart muscle is not getting enough oxygen-rich blood for a short period of time. The mammalian heart is an aerobic organ and a regular supply of oxygen is indispensable to maintain cardiac function and viability. For this reason heart tissue is extremely sensitive to oxygen deprivation and relatively short periods of ischemia and subsequent reperfusion lead to cell death. The inadequate blood flow is caused by total or

partial obstruction of the coronary arteries (Opie 1998). When the coronary arteries cannot supply enough oxygen-rich blood to the heart symptoms of myocardial ischemia can occur. Actually cardiovascular disease and the resulting cardiac ischemia is a most important cause of heart failure worldwide (Lakatta and Sollott, 2002).

Myocardial ischemia is a complex phenomenon affecting the mechanical, electrical, structural and biochemical properties of the hearth. When blood flow is restricted the supply of oxygen to the respiratory chain fails. During ischemia cardiac cells can maintain ATP levels by glycolysis but accumulate glycolytic by-products (lactate, H^+) that cause a decrease in cytoplasmic pH; this condition can damage cardiac cells irreversibly (Solaini and Harris, 2005).

Paradoxically, the major injure to ischemic cells comes on the re-introduction of oxygen (reperfusion). During reperfusion, electrons transfer and ATP synthesis start again and the cytoplasmic pH is restored to 7.0. Nevertheless, this leads further deterioration of cell function with membrane damage followed by cell death (Piper ***et al.***, 2004).

The heart is able to develop natural protection against ischemic injury through a variety of defensive responses triggered by different stimuli. Procedures recognized to stimulate cardioprotection include exercise (Locke et al. 1995), ischemic preconditioning (Hutter et al. 1994), oxidative stress (Sharma and Singh ,2001), and certain pharmacological treatments. However, the preconditioning response of the myocardium may be reduced with ageing

(Abete et ***al.*** 2000; Schulman et ***al***. 2001; Broderick et ***al.*** 2001). A decreased capacity of the myocardium to tolerate an hypoxic stress during ageing has been observed (Starnes ***et al***. 1997, Mariani ***et al***. 2000). In addition, ageing decreases myocardial tolerance to specific features of ischemic injury, including oxidative stress (Abete ***et al.***, 1999).

4.1 Ferritin and ischemic heart disease

Oxygen radical production may significantly contribute to myocardial damage during ischemia/reperfusion injury. While in the absence of Fe^{2+} hydroxyl radicals are relatively slowly formed (Haber-Weiss reaction), the reaction rate is greatly enhanced in the presence of Fe^{2+} (Fenton reaction). In this context, it is of interest to note that use of Fe-chelators reduce myocardial infarction size subsequent ischemia/reperfusion injury.

Beneficial effects of ferritin protein with respect to the ischemia/reperfusion injury could be explained either by an increase of the myocyte storage capacity for ferric iron, or by an increase of the enzymatic activity of ferritin (ferroxidase activity) that reduces the availability of Fe^{2+} for free radical production (Ponka ***et al.*** 1998, Torti and Torti 2002). These effects might be achieved if the ferritin levels in myocardium during ischemia increase.

4.2 Ferritin synthesis regulation during ischemia

Tissue ischemia and cellular hypoxia have been studied in various conditions and changes in ferritin synthesis are well documented. In particular, it has been reported that hypoxia induces ferritin synthesis in rat oligodendrocytes and human oligodendrogliomas (Qi *et al*., 1995). Similar effects were observed in a rat model of acute hypoxic/ischemic insult (Chi *et al*., 2000; Cheepsunthorn *et al*., 2001). Ferritin expression changes during hypoxia are in part mediated by IRPs RNA-binding activity. In fact, a modulation of IRPs activity has been reported during hypoxia/ reoxygenation in epithelial cells (Hanson ***et al.,*** 1999; Schneider and Leibold 2003), in rat hepatoma cells (Hanson and Leibold, 1998), in mouse macrophages (Kuriyama ***et al.***, 2001) and in some mammalian tissues (Meyron-Holtz ***et al.,*** 2004). In contrast, IRP2 activity was found to increase under similar conditions (Toth ***et al.,*** 1999). Finally, more recently a divergent modulation of IRPs activity and ferritin biosynthesis by hypoxia/reoxygenation has been reported in neurons and glial cells (Irace ***et al.,*** 2005).

The phase of reperfusion after ischemia is critical and in many tissues, as heart and brain, the oxidant damage is considerable. During post-ischemic reoxygenation of rat liver, early ferritin degradation was counteracted by enhanced ferritin transcription and simultaneous IRP down-regulation. It was

suggested that this might act to re-establish ferritin levels and limit reperfusion damage (Tacchini *et al*., 1997).

AIM OF RESEARCH

5.1 Aim of the research

In the cardiac ischemia hypoxia and free iron appear to interact in causing the cellular death. Ischemia and re-establishment of blood flow cause the generation of reactive oxygen species catalysed by intracellular free iron with deleterious effects in post-ischemic reperfused tissue.

The aim of this research has been to investigate the molecular mechanisms involved in the regulation of iron metabolism in cardiomiocytes exposed to hypoxia/reoxygenation and evaluate the relationships with cell viability parameters.

MATERIALS AND METHODS

6.1 Cell cultures

The rat embryonic ventricular myocardial cell line H9c2 was purchased from American Type Culture Collection. Cells were cultured in Dulbecco's modified Eagle's medium (DMEM) containing 4.5 g/L glucose and supplemented with 10% fetal bovine serum (FBS), L-glutamine (2 mM), penicillin (100 units/mL) and streptomycin (100

g/mL). Cells were cultured at 37°C in a humidified 5% CO2 atmosphere. Cells were cultured to ~90% confluence before experimental procedures.

6.2 Combined oxygen, glucose and serum deprivation and reoxygenation

The H9c2 cells were exposed to oxygen, glucose and serum deprivation (OGSD) for different times. Briefly, the culture medium was replaced with deoxygenated (saturated for 10 min. with 95% N_2 and 5% CO_2) glucose-free Earle's balanced salt solution containing NaCl 116 mM, KCl 5.4 mM, $MgSO_4$ 0.8 mM, $NaHCO_3$ 26.2 mM, NaH_2PO_4 1 mM, $CaCl_2$ 1.8 mM, glycine 0.01 mM

and 0.001 w/v phenol red. Cultures were then placed in an humidified 37°C incubator inside an anaerobic chamber containing a gas mixture of 95% N_2 and 5% CO_2. Reoxygenation was achieved by replacing the OGSD medium with oxygenated regular medium containing glucose and serum and returning cultures to normoxic conditions (37°C in a humidified 5% CO_2 atmosphere) for various times (3h and 24h).

6.3 Cell viability assay

Cell viability was evaluated by measuring the level of mitochondrial dehydrogenase activity using 3-(4,5-dimethyl-2-thiazolyl)-2,5-diphenyl-2H-tetrazolium bromide (MTT) as substrate. The assay was based on the redox ability of living mitochondria to convert dissolved MTT into insoluble formazan. Briefly, after OGSD and OGSD/Reoxy, the medium was removed and the cells were incubated in 20 µl of MTT solution (0.5 mg/mL) for 1 h in a humidified 5% CO2 incubator at 37°C. The incubation was stopped by removing the MTT solution and adding 100 µl of DMSO solution to solubilize the formazan. The absorbance was monitored at 540 nm by using a Perkin-Elmer LS 55 Luminescence Spectrometer (Perkin-Elmer Ltd, Beaconsfield, UK). The data are expressed as the percentage of cell viability to control cultures.

6.4 Evaluation of living/dead cells

The relative number of live and dead cells in cultured cell populations was evaluated through the simultaneous measure of two protease activities using the MultiTox-Fluor Cytotoxicity Assay (Promega Corporation). The assay use two fluorogenic substrates (live cell reagent and dead cell reagent) supplied as DMSO solutions. The substrates are differentially cleaved in live and dead cells to yield the fluorescent products AFC and R110. AFC and R110 have sufficiently different excitation and emission wavelengths to allow the measure in the same mixture. The AFC signal increases with increasing cell viability and the R110 signals increases as the number of dead cells increases. By monitoring the AFC and R110 signals the ratio of live to dead cells in a cell population can be determined. The MultiTox-Fluor Cytotoxicity Assay can be performed in 96- well plates without additional washing or cell harvesting steps.

6.5 Cellular energetic state

The intracellular levels of ATP were determined using a test of bioluminescence (Bioluminescent somatic cell assay kit, Aldrich Sigma, St.

Louis USA). Such method uses the luciferase enzyme that catalyzes the oxidation of the luciferin involving adenosine triphosphate (ATP) and produce a luminous light with intensity proportionl to the cellular ATP.

The cells were resuspended in PBS to the concentration of 10^6 cellule/mL. To 50 µL of such suspension were added 50 µL of sterile water and 100 µL of buffer (Somatic Cell Releasing Reagent) to allow the instantaneous release of cellular ATP. Successively, 100 µL of ATP mix assay to 100 µL of sample were added and the intensity of the luminous emission was measured by luminometer. The results are expressed as percentage respect to the control and were standardized for number of cells.

6.6 Measurement of ROS

The formation of ROS was evaluated using the probe 2',7'-dichlorofluorescin-diacetate (H2DCF-DA) as described (LeBel ***et al***., 1992). Briefly, H9c2 cells were grown in DMEM containing 10% (v/v) fetal bovine serum and subsequently were plated at a density of 20.000 cells/well into 96-well. Cells were cultured for 24 h and then incubated in medium containing 50 µM of H_2DCF-DA (Sigma) for 1 h at 37 °C.

H_2DCF-DA is a non-fluorescent permeant molecule that passively diffuses into cells, where the acetates are cleaved by intracellular esterases to form H_2DCF.

In the presence of intracellular ROS, H_2DCF is rapidly oxidized to the highly fluorescent 2',7'-dichlorofluorescein (DCF). Cells were washed twice with PBS buffer and then were treated with deoxygenated, serum and glucose-free Earle's balanced salt solution for various times. After treatment, cells were washed twice with PBS buffer and the dishes were positioned in a fluorescent microplate reader (Perkin Elmer LS 55 Luminescence Spectrometer, Perkin-Elmer Ltd., Beaconsfield, England). Fluorescence was monitored using an excitation wavelength of 485 nm and an emission wavelength of 538 nm.

6.7 Lipid peroxidation assay

Lipid peroxidation products in the cells were measured by the thiobarbituric acid colorimetric assay (Esterbauer and Cheeseman, 1990). Briefly, after OGSD and OGSD/Reoxy cells were washed and collected in PBS Ca^{2+}/Mg^{2+} free medium containing 1 mM EDTA and 1.13 mM butylated hydroxytoluene (BHT). Cells were broken up by means of sonicator. Trichloroacetic acid, 10% (w/v), was added to cellular lysate and, after centrifugation at 1,000g for 10 min., the supernatant was collected and incubated with 0.5 % (w/v) thiobarbituric acid at 80°C for 30 min. After cooling, malondialdehyde (MDA) formation was recorded (A530 nm and A550 nm) in a Perkin Elmer LS-55 spectrofluorimeter. Samples were scaled for protein concentration determined

by the Bio-Rad protein assay and a standard curve of MDA was used to quantify the MDA levels formed during the experiments. The results are presented as percentage of MDA production versus a control obtained in untreated cultures.

6.8 LDH assay

Cytosolic levels of LDH in the extracellular medium were measured by using an LDH assay Kit from Promega. The CytoTox-ONE™ Assay rapidly measures the release of lactate dehydrogenase (LDH) from cells with a damaged membrane. The CytoTox-ONE™ Reagent mix does not damage healthy cells, therefore the reaction can be performed directly in wells containing a mixed population of viable and damaged cells. Production of fluorescent resorufin product is proportional to the amount of LDH.

Assay plates are allowed to equilibrate to ambient temperature, and CytoTox-ONE™ Reagent is added to each well and incubated for 10 minutes. Stop Solution is added, and the fluorescent signal is measured. The amount of fluorescence produced is proportional to the number of lysed cells. Briefly, after induction of OGSD and OGSD/reoxygenation, the medium was removed and LDH content was evaluated by measuring the fluorescence in a microplate reader (Perkin Elmer LS 55 Luminescence Spectrometer, Perkin- Elmer Ltd.,

Beaconsfield, England). using an excitation wavelength of 560 nm and an emission wavelength of 590 nm.

The results were expressed as percentage of LDH released versus untreated cell cultures.

6.9 Preparation of cytosolic extracts

After OGSD and OGSD/Reoxy treatment H9c2 cells were washed and scraped off with PBS containing 1 mM EDTA. To obtain cytosolic extracts for electrophoretic mobility shift assay (EMSA) cells were treated with lysis buffer containing 10 mM HEPES, pH 7.5, 3 mM $MgCl_2$, 40 mM KCl, 5% (v/v) glycerol, 1 mM dithiothreitol (DTT), 0.2% (v/v) Nonidet P-40 (NP-40) and protease inhibitor tablet (Roche, Mannheim, Germany) at 4°C. Cell debris and nuclei were pelleted by centrifugation at 15,000 g for 10 min. at 4°C and supernatants were stored at –80°C. For Western blot analysis cells were collected by scraping and low-speed centrifugation. Cell pellets were lysed at 4°C for 1 h in a buffer containing 10 mM KCl, 1.5 mM $MgCl_2$, 20 mM HEPES, pH 7.5, 1 mM EDTA, 1 mM DTT, 0.1 mM phenylmethylsulphonyl fluoride and proteases inhibitors tablets (Roche). The protein concentration was determined by the Bio-Rad protein assay according to the supplier's manual (Bio-Rad, Milan, Italy).

6.10 Electrophoretic mobility-shift assay (EMSA)

Plasmid pSPT-fer, containing the sequence corresponding to the IRE of the H-chain of human ferritin, linearized at the Bam HI site, was transcribed *in vitro* with T7 RNA polymerase (Promega). The transcriptional reaction was performed at 38.5 °C for 1 h with 200 ng of plasmid in the presence of 50 μCi of [α-^{32}P] CTP (800 Ci/mM) (Amersham Biosciences) and 0.5 mM ATP, GTP and UTP (Promega), in 20 μl reaction volume (Festa ***et al.,*** 2000). The DNA template was digested with 10 units of RNase-free DNase I for 10 min at 37 °C. Free nucleotides were removed on Sephadex G-50 column (Roche). For RNA-protein band-shift analysis, cytosolic extracts (5 μg) were incubated for 30 min. at room temperature with 0.2 ng of *in vitro* transcribed ^{32}P-labeled IRE RNA. The reaction was performed in buffer containing 10 mM HEPES, pH 7.5, 3 mM $MgCl_2$, 40 mM KCl, 5% (v/v) glycerol, 1 mM DTT and 0.07% (v/v) NP-40, in a final volume of 20 μL. To recover total IRP1 binding activity, cytosolic extracts were pre-incubated for 10 min with 2-mercaptoethanol at a 2% (v/v) final concentration, before the addition of ^{32}P-labeled IRE RNA. Unbound RNA was digested for 10 min. with 1 unit of RNase T_1 (Roche) and non specific RNA-protein interactions were displaced by the addition of 5 mg/mL heparin for 10 min. RNA-protein complexes were separated on 6% non denaturing polyacrylamide gel for 2 h at 200 V. After electrophoresis, the gel was dried and autoradiographed at –80°C. The IRP-IRE complexes were

quantified with a GS-700 imaging densitometer and/or with a GS-505 molecular imager system (Bio-Rad). The results are expressed as the percentage of IRP binding activity versus 2-mercaptoethanol-treated samples.

6.11 Western blot analysis

Samples containing 50 or 100 μg of proteins were denatured, separated on a 12% (for ferritin and caspase-3) or 8% (for IRP1 and TfR) SDS-polyacrylamide gel and electro-transferred onto a nitrocellulose membrane (Amersham Biosciences, UK) using a Bio-Rad Transblot. Proteins were visualized on the filter by reversible staining with Ponceau-S solution (Sigma) and destained in PBS. Subsequently the membranes were blocked at 4°C in milk buffer (1X PBS, 10% (w/v) non fat dry milk, 0.2 % (v/v) Tween 20) overnight and then incubated for 3 h at room temperature with 1:1000 rabbit polyclonal antibody to human ferritin (DakoCytomation, Glostrup, Denmark), or with1:1,000 mouse antibody to human transferring receptor-1 (Zymed Laboratories Inc., CA, USA), or with 1:250 goat antibody to human IRP1 (Santa Cruz Biotechnology, Inc., Santa Cruz, CA, USA) or with 1:2000 rabbit polyclonal antibody caspase-3 (Calbiochem).

Subsequently, the membranes were incubated for 90 min at room temperature with peroxidase-conjugated goat anti-mouse IgG+IgM, or peroxidase-

conjugated rabbit anti-goat IgG, or peroxidase-conjugated goat anti-rabbit IgG (all the secondary antibodies were purchased

from Jackson ImmunoResearch Laboratories, Baltimore Pike, West Grove, PA). The resulting complexes were visualized using chemoluminescence Western blotting detection reagents (ECL, Amersham Biosciences). The optical density of the bands was determined by a GS-700 imaging densitometer (Bio-Rad). Normalisation of results was ensured by incubating the nitrocellulose membrane in parallel with the β-actin antibody.

6.12 RNA extraction

After OGSD and OGSD/Reoxy treatments, total cellular RNA was isolated from cells by the TRIzol reagent (Invitrogen Life Technologies, Carlsbad, CA) extraction method. The TRIzol reagent is a ready-to-use for the isolation of total RNA from cells. Briefly, cells grown in monolayer were lysed directly in culture dish by adding 1 mL of TRIzol reagent to a 3.5 cm diameter dish, and passing the cell lysate several times through a pipette. The homogenized samples were incubated for 5 min at room temperature to permit the complete dissociation of nucleoprotein complexes. 200 μL of chloroform were added to each sample and tubes were shaked vigorously for 15 seconds and then incubated for 3 min at room temperature. Successively, samples were

centrifuged at 12,000g for 15 min at 4°C. Following centrifugation, RNA remains exclusively in the aqueous phase and was precipitated with isopropyl alcohol. After centrifugation at 12,000 g at 4°C for 15 min, RNA precipitate was resuspended in sterile water and quantified.

6.13 Northern blot analysis

For Northern blot analysis 25 μg of total RNA were fractionated on a 1.5% agarose denaturing formaldehyde gel in MOPS buffer. RNA was transferred by blotting in 20X SSC (1X SSC, 0.15 M NaCl, 0.015 M Na-citrate), pH 7.0, to Hybond-N filters (Amersham Biosciences). A cDNA fragment corresponding to human cDNA for H-ferritin was ^{32}P-radiolabelled using the random priming method (Amersham Biosciences) and α-^{32}P dCTP, 3000 Ci/mM (Amersham Biosciences). The reaction was stopped by adding 0.5 μL EDTA 0.5 M and probe was purified on a Bio-Spin 30 chromatography column (Bio-Rad). The hybridization was performed for 18 h at 65°C in 0.5 M sodium phosphate buffer, pH 7.2, 1 mM EDTA, pH 8.0, 7% (w/v) SDS. The filters were washed in 0.05 M sodium phosphate buffer pH 7.2, 1% (w/v) SDS at 65°C and autoradiographed at –80 °C. The ethidium bromide-stained RNA gel was used

as control for RNA loading. The bands corresponding to H-ferritin mRNA were quantified by densitometry and the results are plotted as arbitrary units.

6.14 RT-PCR analysis

The levels of TfR mRNA were evaluated by using PCR amplification of reverse-transcribed mRNA. The housekeeping gene β-actin was used as an internal control. Total RNA was reverse-transcribed into cDNA by using the random priming method and Superscript III-Reverse Transcriptase (Invitrogen). cDNA was amplified by PCR using Taq-Polymerase (Invitrogen) according to the manufacturer's instructions.

The primers for TfR were:

sense 5′- TTCCTCATGTAAGCTGGAAC-3′,

antisense 5′-ACGTCCTGCATTATCTTCGC-3′.

The primers for β-actin were :

sense 5′-ATGAAGATCCTGACCGAGCGT-3′,

antisense 5′-AACGCAGCTCAGTAACAGTCCG-3′.

The amplified fragments were 509 bp and 584 bp, respectively. The PCR reaction was performed under the following conditions: a first cycle of denaturation at 94 °C for 1 min 40 s, then 30 cycles of denaturation at 94 °C for 40 s, annealing at 52 °C for 40 s, extension at 72 °C for 1 min and one additional cycle of extension at 72 °C for 8 min. The PCR products were run on 1% agarose gel and stained with ethidium bromide. The signals were quantified by laser densitometry and values normalized to β-actin levels.

6.15 Statistical Analysis

For the determination of vitality parameters the results are expressed as mean $\pm$ standard error of the mean (SEM) of n observations, where n represents the number of experiments performed. All experiments were performed in triplicate. The results were analysed by one-way ANOVA followed by a Bonferroni post hoc test for multiple comparisons. A P-value less than 0.05 was considered significant. The densitometric data of EMSA, Western blot, Northern blot and RT-PCR analysis are reported as means $\pm$ SEM. Statistical significance among the means was determined by the ANOVA followed by the Newman-Keuls test. A p value ≤ 0.05 was considered statistically significant.

7. RESULTS

7.1 Effects of OGSD/reoxygenation on cellular vitality and survival

In myocardial ischemia the reduced blood supply to the cardiac muscle can induce cellular injure with possible induction of necrosis or apoptosis. We have evaluated the effects of the oxygen, glucose and serum deprivation (OGSD) on cellular vitality and survival in our model of cardiac ischemia *in vitro*. To investigate the effects of OGSD/reoxygenation on cell survival, we have analyzed cell vitality and cell membrane damage. Cell viability was examined by measuring the mitochondrial redox capacity with the MTT assay. H9c2 cells were exposed to hypoxic conditions for 30 minutes to 12 hours and successively to normoxic conditions for 3h and 24h. As shown in Fig. 9 the H9c2 cells are particularly responsive to the deprivation of oxygen and metabolic nutrients. The hypoxia induces a progressive impairment of mitochondrial oxidative capacity with a decrease of cellular vitality of about 50% when the cells were exposed to OGSD for 6h. After hypoxic conditions, when oxygen supply is restored (reoxigenation of 24h) the mitochondrial redox activity resulted almost normal. When the cells were exposed to long-term hypoxic conditions (12h), an enhanced mitochondrial activity impairment was evident also during the reoxigenation.

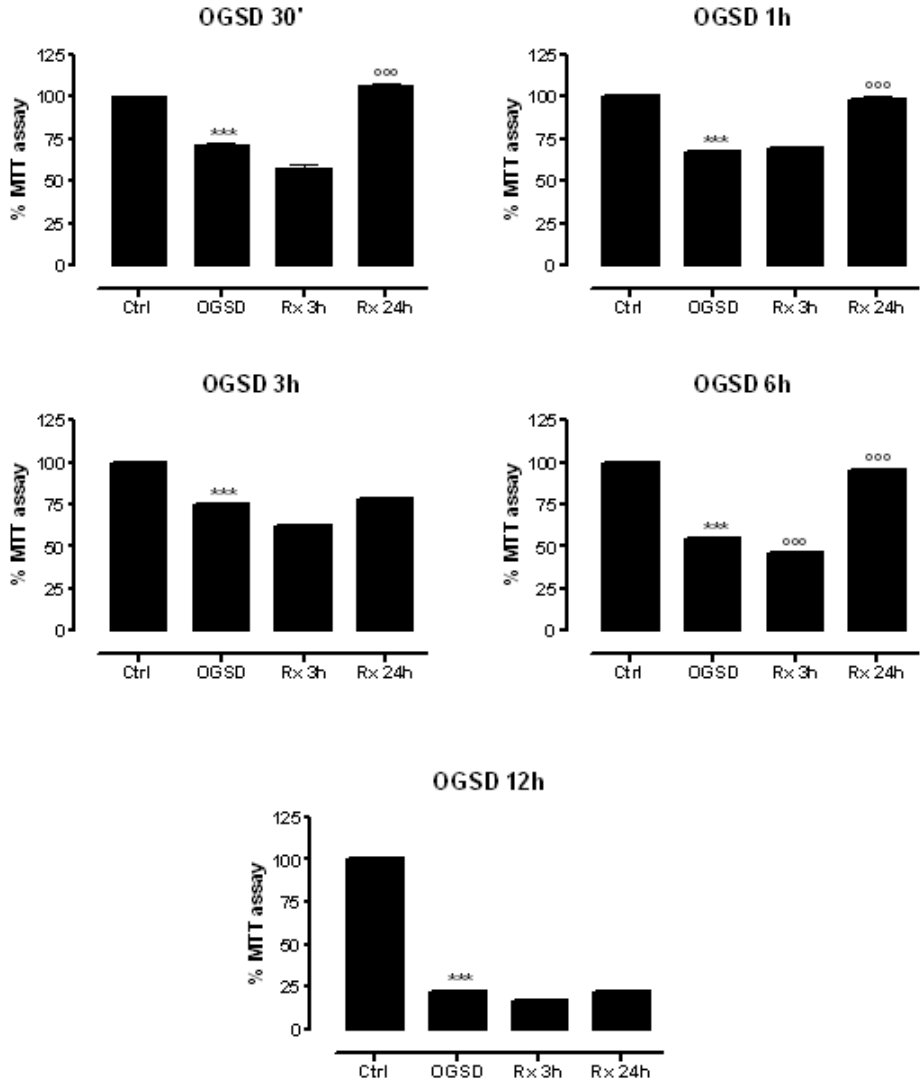

Fig.9. Cell vitality during OGSD/reoxigenation
The survival of H9c2 cells during OGSD/reoxigenation was evaluated by MTT assay measuring the mitochondrial dehydrogenases activity. (*** $p<0.001$ *vs* Ctrl; °°° $p<0.001$ *vs* OGSD)

The determination of living or dead cells on a total cell sample was performed using a fluorimetric method. The obtained results, reported in table 1, showed a

progressive and constant reduction of the percentage of the living cells in agreement with to the time of OGSD (30 minutes, 1h, 3h, 6h). The hypoxia of 12h causes the death of about 70% of the cells, whereas the reoxigenation induces the death of about 85% of the cells. Brief-term hypoxic conditions did not drastically affect cells viability.

On the basis of cellular vitality and survival results we suppose that in our experimental conditions the hypoxia of 6h is the "point of no return", beyond which the cell is devoted to die and can't revert to normal conditions.

OGSD (time)	OGSD	Rx 3 h	Rx 24 h
0.5 h	87 ± 5%	85 ± 6%	87 ± 5%
1 h	80 ± 5%	75 ± 5%	80 ± 6%
3 h	60 ± 6%	50 ± 5%	50 ± 5%
6 h	50 ± 5%	45 ± 7%	45 ± 6%
12 h	30 ± 5%	22 ± 5%	15 ± 5%

Table 1. Evaluation of living/dead cells after OGSD/reoxygenation

7.2 Energetic state of cells during OGSD/reoxygenation

Successively, we have analyzed the energetic state of cells by determination of ATP levels, measured using a bioluminescent method. The cells were exposed

to hypoxic conditions for 30 minutes to 12 hours and then to normoxic conditions for 3h and 24h. The observed intracellular ATP levels are in agreement with the mitochondrial redox activity. In fact, exposure to OGD for 3h and mostly for 6h caused a reduction of the ATP levels, however during the reoxygenation phases the ATP levels gradually returned to baseline levels (Fig. 10). Hypoxia exposure prolonged (12h) led to a decrease of the intracellular ATP levels, that can't revert to normal conditions during reoxigenation.

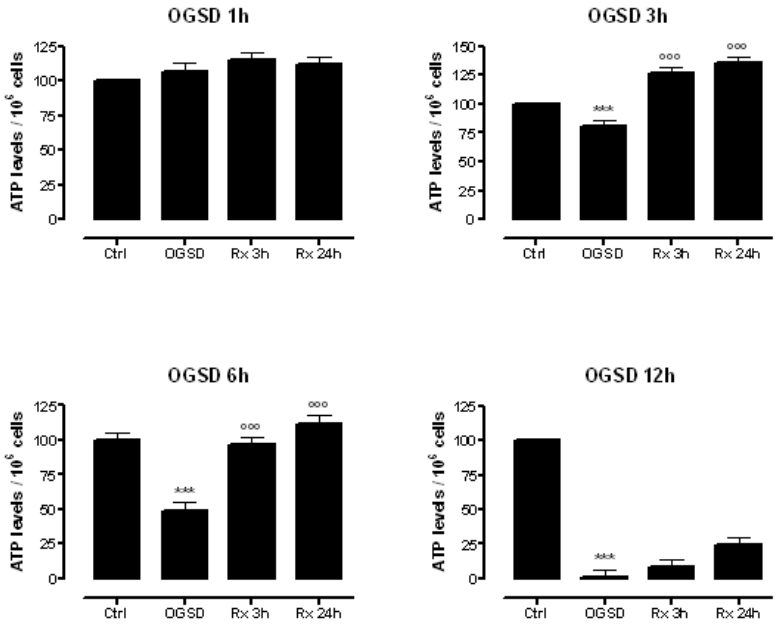

Fig.10. **ATP levels evaluation**
The energetic state of the H9c2 cells after OGSD/reoxigenation was evaluated by determination of the ATP levels using a bioluminescent analysis.
(*** $p<0.001$ *vs* Ctrl; °°° $p<0.001$ *vs* OGSD).

7.3 Oxidative stress in cardiac ischemia/reperfusion injury

The ROS are supposed to play a significant role in tissue ischemia and reperfusion injury and several studies have demonstrated that during cardiac ischemia/reperfusion there is oxidative stress. To monitor the oxidative stress status in our experimental conditions we evaluated the ROS production by means of the fluorescent dye H_2DCF-DA and lipid peroxidation by measurement of MDA production. As reported in Fig. 11 the hypoxic condition of 3h was associated with a mild increase of ROS production both during hypoxia and reoxigenation.

Whereas there is a significant increase of the ROS levels after hypoxic conditions of 6h that remains constant during the early reoxigenation phase.

Lipid peroxidation products from cells were measured by the thiobarbituric acid colorimetric assay that quantifies malondialdehyde

(MDA) levels. As reported in Fig. 12 OGSD did not appreciably enhance the MDA production, whereas a significant increase of lipid peroxidation (about 80%) was evident during the early reoxigenation phase.

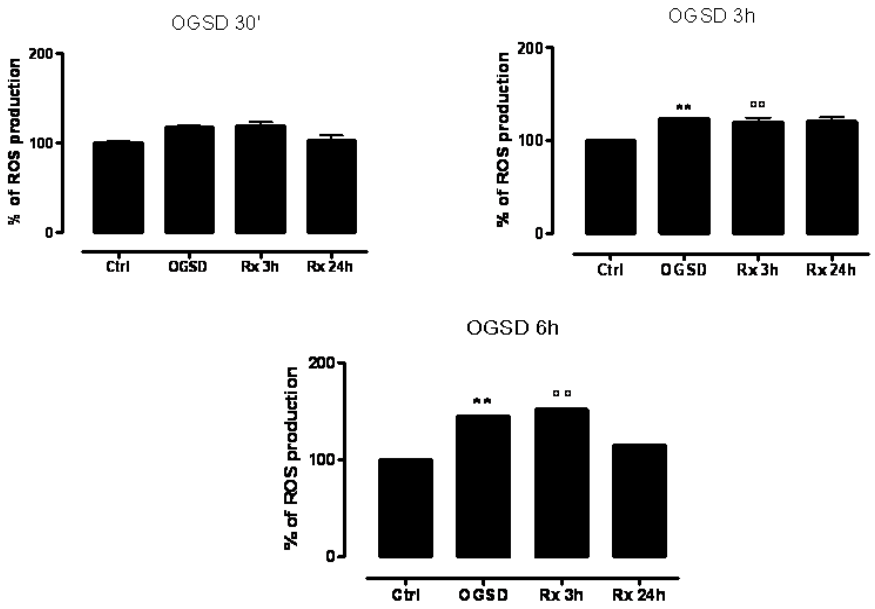

Fig.11. ROS production

Measure of ROS levels performed with the H_2DCF-DA in H9c2 cells after OGSD/reoxigenation treatments.

(** p<0.001 *vs* Ctrl; °° p<0.001 *vs* OGSD).

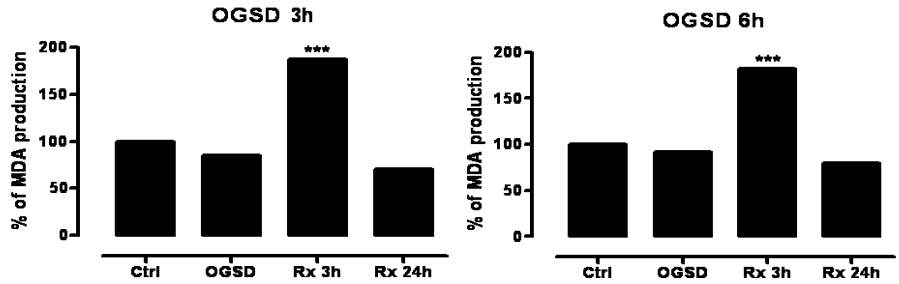

Fig. 12. Lipid peroxidation after OGSD/reoxigenation

Lipid peroxidation was measured by a thiobarbituric acid colorimetric assay and the data are presented as percentage of MDA production versus a control.

(*** p<0.001 *vs* Ctrl).

7.4 Cardiac cells exposed to OGSD/Reoxygenation die through necrosis or apoptosis?

There are diverse ways for a cell to die. Apoptosis is a tightly regulated energy-dependent process in which cell death follows a programmed set of events. Necrosis is a form of cell-death that results from acute tissue injury and provokes an inflammatory response.

To evaluate the effects of OGSD/reoxygenation on cellular death we analyze the expression of caspase-3, an hallmark of apoptosis. Figure 13 shows the result of western blot analysis for caspase 3 cleavage. It is evident that the exposure of cardiac cells to hypoxia/reoxigenation doesn't induce activation of caspase-3, suggesting a death by necrosis.

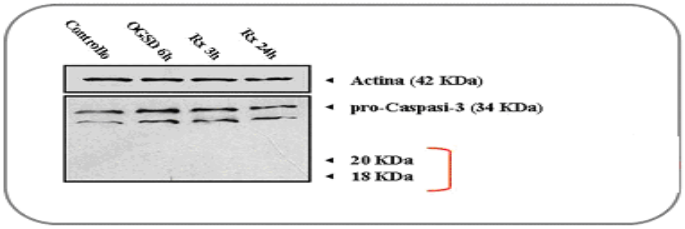

Fig. 13. Western blot analysis for caspase-3
H9c2 cells were exposed to OGSD for 6 h followed by reoxygenation (3h and 24h). Western blot analysis was performed using caspase-3 antiserum. The anti-β-actin antibody was used to standardize the amounts of proteins in each lane.

These results was supported by the measurement of cytoplasmic lactate dehydrogenase (LDH) release. Cell injury was assessed by measuring the amount of lactate LDH released into the medium after OGSD and OGSD/reoxigenation. The percent of LDH release was calculated from the minimum LDH release (0%) from untreated cells. As shown in Figure 14 hypoxia exposure from 30 minutes to 6h did not induce LDH release, while long-term hypoxic conditions (12h) causes cell membrane damage and induce LDH release.

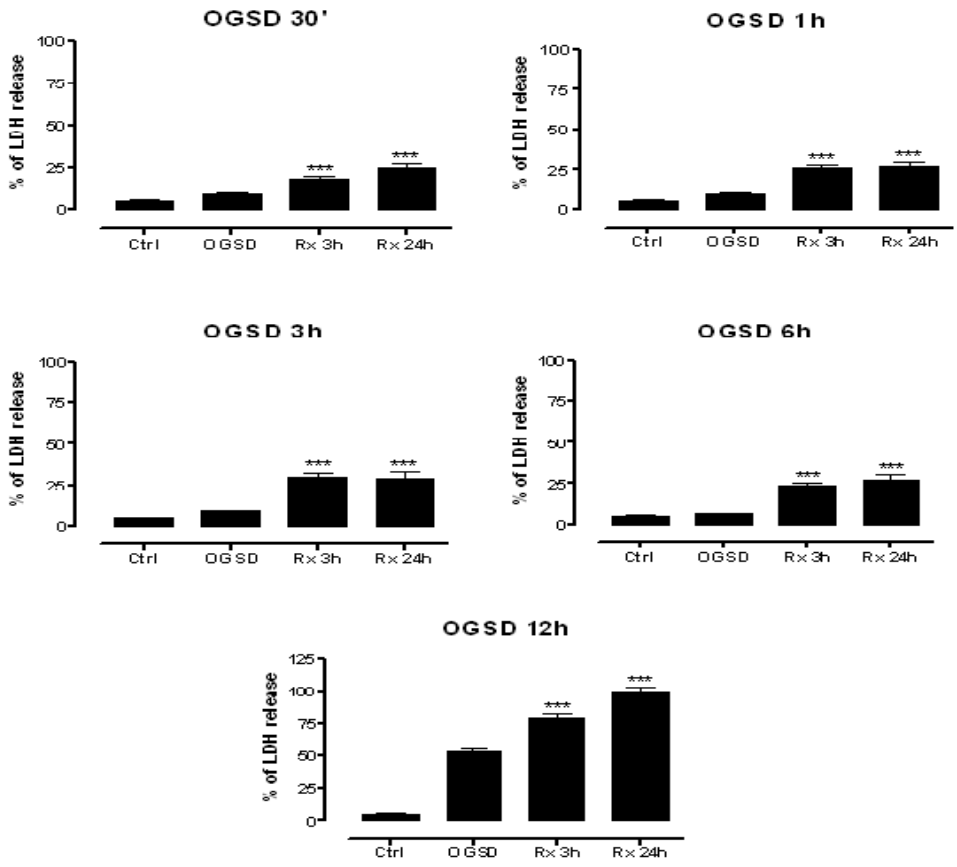

Fig.14. Measure of LDH release
Lactate dehydrogenase (LDH) release evaluated in H9c2 cells after OGSD/reoxigenation exposure. (*** $p<0.001$ *vs* Ctrl).

7.5 Iron Regulatory Proteins activity and expression during OGSD /reoxygenation

To determine the effects of OGSD on IRP RNA-binding activity, we exposed H9c2 cells to normoxic and hypoxic conditions for 30 minutes to 12 h and then we measured the IRP RNA-binding activity by RNA band-shift assay. As

shown in Fig. 15 in cardiac cells OGSD caused a decrease IRP1 RNA-binding activity. This effect already appeared after only 30 min of OGSD exposure and persisted up to 12 h (data not showed). In conjunction with the IRP1 RNA-binding decrease, there was an OGSD-dependent increase in IRP2 RNA-binding activity. The reoxygenation reverted OGSD-induced IRP1 modulation and IRP1-RNA binding activity increased after 3 h of reoxygenation and baseline levels generally were reached after 24 h of reoxygenation.

To determine the total amount of IRP1 RNA-binding activity, β-mercaptoethanol was added to the binding reactions before the addition of ^{32}P-labeled IRE probe. β-mercaptoethanol reveals "latent" IRP1 RNA-binding activity thus giving the total amount of IRP1 activity (100% of IRE-binding).

To evaluate whether the modulation of IRP-1RNA binding activity was caused by a variation of IRP-1 protein content, we successively

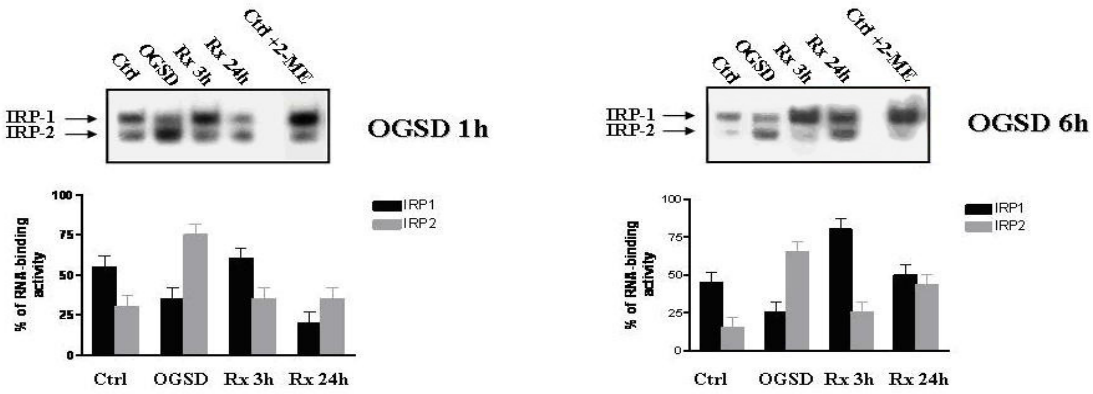

Fig. 15. IRP1 and IRP2 RNA-binding activity in H9c2 cells during OGSD/reoxygenation
EMSA was performed in the absence or presence of 2% β-mercaptoethanol (2-ME). H9c2 cells were exposed to normoxic or hypoxic conditions for 1h and 6h followed by exposure to normoxia for 3 and 24h. RNA-protein complexes were separated on non-denaturing 6% polyacrylamide gels and revealed by autoradiography. IRP1-RNA complexes were quantified by densitometric and/or PhosphorImager analysis. The results were plotted as percent of respective control treated with 2-ME.

analysed the IRP-1 levels in H9c2 cells exposed to OGSD/reoxygenation for the indicated times.

As shown in Figure 16) immunoblot analysis did not show any appreciable variations in the amounts of IRP-1 protein , suggesting that OGSD-induced IRP1 modulation was not due to a variation in IRP1 protein levels.

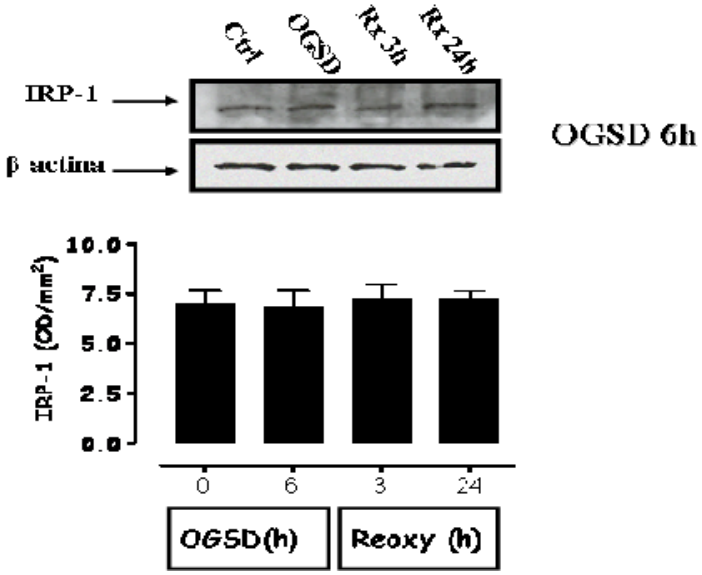

Fig.16. **Western blot analysis of IRP-1 protein**
H9c2 cells were exposed for 6 h to OGSD followed by reoxygenation for 3 h and 24 h. Equal amounts of proteins (100 μg) were separated on a 8% SDS–polyacrylamide gel and subjected to Western blot analysis using IRP-1 antiserum. β-actin was used as internal control to standardize the amounts of proteins in each lane.

7.6 Effects OGSD/reoxigenation on transferrin receptor expression

To evaluate the effect of OGSD/reoxygenation on TfR expression, we determined TfR protein levels by Western blot analysis on lysates obtained from H9c2 cells after 3h and 6h of OGSD followed by 3h and 24 h of reoxygenation. As shown in Figure 17, the hypoxic condition induce a reduction of TfR content, while there was a significant increase in TfR content in the late phase of reoxygenation (24 h). Interestingly, the reoxygenation-

induced increase of TfR content was more evident after an hypoxic exposure of 6h.

To assess whether the TfR level variation observed during OGD and OGD/reoxygenation might result from transcriptional control, we analysed the levels of corresponding mRNA. As shown in Figure 18, the level of TfR mRNA, analysed by RT-PCR, was slightly decreased after the OGD period and progressively increased during the reoxygenation phases (3 and 24 h).

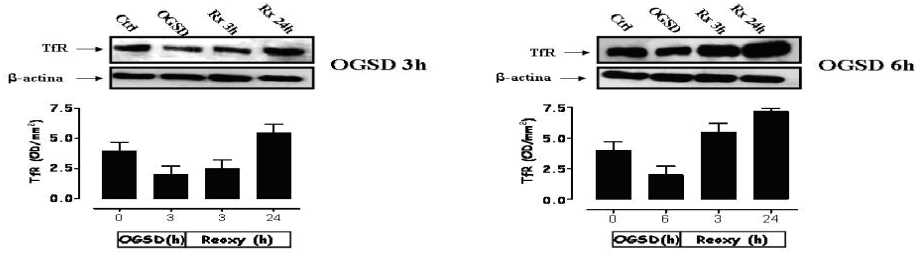

Fig.1

7. **Western blot analysis of TfR protein**

Equal amounts of cytosolic lysates containing 100 µg of proteins, were fractionated by 8% SDS–PAGE and subjected to Western blot analysis using TfR-1 antiserum. Immunocomplexes were detected by chemoluminescence. The anti-β-actin antibody was used to standardize the amounts of proteins in each lane.

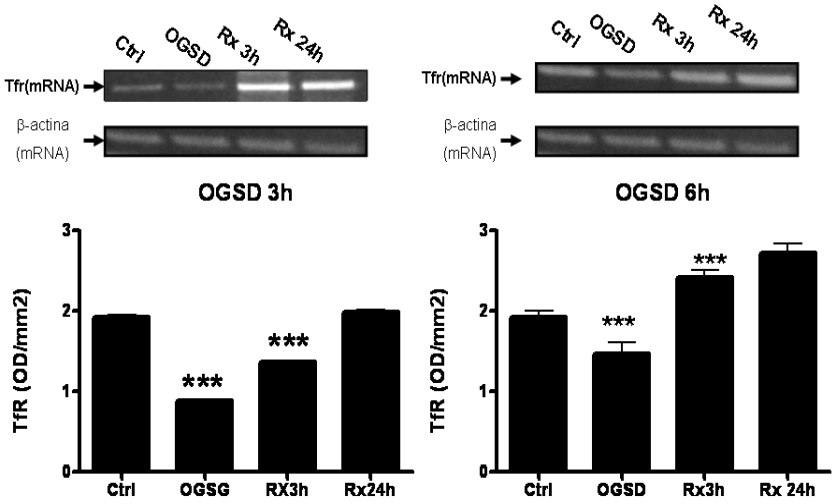

Fig.18. TfR mRNA expression.
RNA was isolated from H9c2 cells exposed for 3h and 6h to OGSD followed by reoxygenation (3h and 24h). 1 μg of total cellular RNA were utilized for RT-PCR. The bands corresponding to TfR mRNAs were quantified by densitometric analysis and the results plotted in a
bar graph. Data were normalized on the basis of β-actin levels mRNA.

7.7 Effects of OGSD/reoxigenation on ferritin expression

To evaluate ferritin expression in H9c2 cells during OGSD and following reoxygenation, we determined the levels of this proteins by Western blot analysis. As shown in Figure 19, ferritin content resulted unchanged after 3h of OGSD, while these levels significantly increased in the early phase of reoxygenation (3h). Similarly, ferritin content remained unchanged in cells exposed to hypoxic conditions for 6h OGD whereas only slightly increased in

the early phase of reoxygenation (24 h). Interestingly, the reoxygenation-induced increase of ferritin content was less evident after an hypoxic exposure of 6h.

To assess whether the ferritin levels variation observed during OGD/reoxygenation might result from transcriptional control, we analysed by northern blot the levels of corresponding mRNA. As shown in Figure 20, the level of H-ferritin mRNA resulted unchanged after short-term hypoxic conditions (3h) and also during the following reoxigenation phases. After hypoxic conditions of 6h the H-ferritin mRNA content slightly decreased and progressively increased during the reoxygenation phases (3 and 24 h).

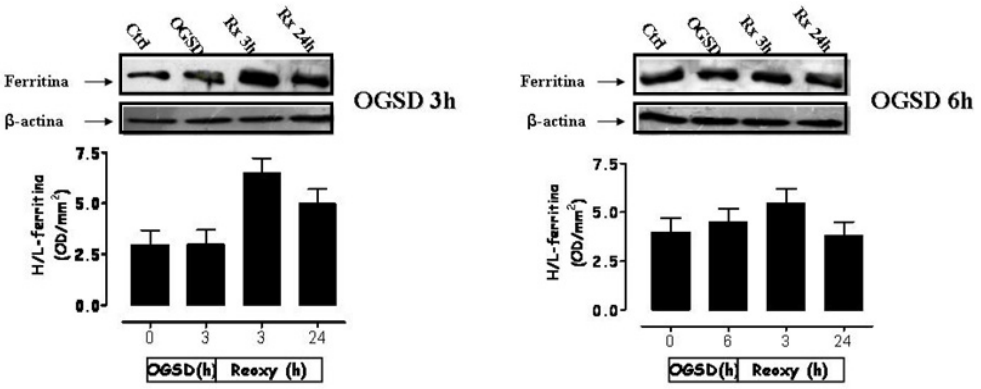

Fig.19. **Western blot analysis of ferritin protein**
Equal amounts of cytosolic lysates containing 50 μg of proteins, were fractionated by 12% SDS–PAGE and subjected to Western blot analysis using ferritin antiserum. Immunocomplexes were detected by chemoluminescence. The anti-β-actin antibody was used to standardize the amounts of proteins in each lane.

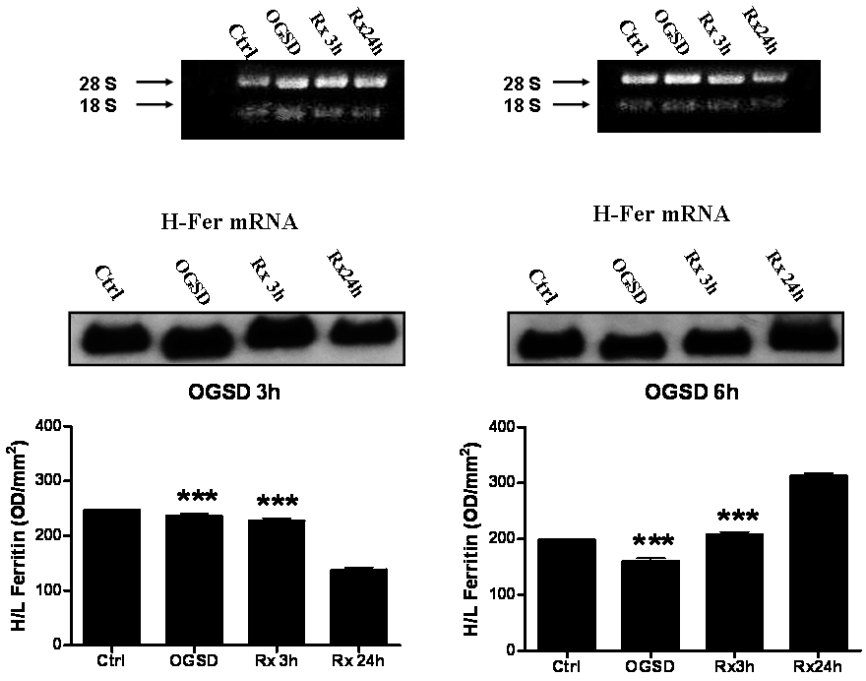

Fig. 20. Ferritin mRNA expression.
30 μg of total cellular RNA were hybridized to H-ferritin cDNA ^{32}P-radiolabelled probe. On the top is shown ethidium bromide-stained RNA gel as control for RNA loading. The bands corresponding to H-ferritin mRNA were quantified by densitometry and the results are plotted as arbitrary units.

DISCUSSION AND CONCLUSIONS

8.1 Discussion and conclusions

Perturbations in cellular iron and ferritin content are emerging as an important elements in the pathogenesis of disease. The changes in ferritin content are important not only in the classic diseases of iron acquisition, transport, and storage, such as primary hemocromatosis, but also in diseases characterized by inflammation, infection, injury, and repair. Among these are some of the most common diseases, as neurodegenerative diseases such as Parkinson disease (Linert *et al*, 2000) and Alzheimer disease (Kondo *et al*, 1996), vascular diseases such as cardiac and cerebral ischemia and reperfusion injury (Chi SI *et al*, 2000), and a variety of premalignant conditions and cancers.

We have demonstrated that oxygen, glucose and serum deprivation followed by reoxygenation (OGSD, OGSD/reoxygenation) affect the viability and survival of H9c2 cardiac cells. In particular, exposure of H9c2 to OGSD/reoxygenation for different times determined impairment of mitochondrial activity. The H9c2 cells are in fact particularly sensitive to the deprivation of oxygen, glucose and serum. The hypoxia caused a progressive reduction of cell viability, inducing a progressive mitochondrial suffering

starting from 30 minutes of OGSD, and leading a decrease of mitochondrial dehydrogenases activity of around 50% after 6h of OGSD. However, the return to normoxic conditions subsequent to OGSD treatment of 6h, induced the almost complete re-establishment of mitochondrial redox capacity.

The prolonged hypoxia (12 h of OGSD) induced a marked mitochondrial suffering, which was not reverted during the subsequent reoxygenation phases. Therefore, in our experimental conditions hypoxia treatment of 6h is considered as the "point of no return"; prolonged exposure to hypoxia lead to cellular permanent damage.

Hypoxia caused a progressive and constant reduction of the percentage of living cells, according to the duration of OGSD. An hypoxic condition of 12h determined approximately the death of about the 70% of the cell population, and the subsequent 24h reoxygenation increased this value to about the 85%.

Similarly, OGSD reduced ATP levels in cardiac cells. In particular, prolonged hypoxia (12 h of OGSD) induced a marked reduction of ATP, which is not reverted by the subsequent reoxygenation, according to the other viability experiments.

To investigate the effects of OGSD and OGSD/reoxygenation on cellular ROS generation, we analyzed the accumulation of ROS and the lipid peroxidation. Short hypoxia treatments and following reoxigenation did not change significantly ROS production in H9c2. On the contrary, 6h of hypoxia was

associated with a significant increase of ROS levels and of lipid peroxidation products.

Generally, in tested "*in vitro*" experimental models of ischemia there are two possible ways in which cells die: apoptosis and/or necrosis. Apoptosis is a form of programmed cell death and involves a series of biochemical events leading to a characteristic cell morphology and death. Exposure of H9c2 cardiac cells to OGSD and to subsequent reoxygenation did not induced activation of caspase-3, one of the main hallmarks of apoptosis, thus suggesting a possible necrotic pathway of death shown by H9c2 exposed to these pathological conditions.

To confirm that in our experimental model ischemic conditions preferentially induced cells death *via* necrosis, we evaluated damages to the cell plasmatic membranes by analyzing LDH release by cells. Short hypoxia did not induced LDH release, while prolonged OGSD treatment induced a dramatically LDH release, thus confirming a necrotic cell death.

With regard to cellular iron homeostasis, IRPs activity appears to be differently regulated in hypoxia and reoxigenation. More in detail, IRP1 binding activity during OGSD was significantly decreased, and this effect appeared already after 30 min of OGSD exposure and persisted up to 12 h of hypoxic treatment. The effect was not caused by a change in IRP1 protein content during OGSD, as demonstrated by western blot experiments. On the contrary, concomitant to the IRP1 RNA-binding decrease, it is possible to observe a slight OGSD-

dependent increase in IRP2 RNA-binding activity. In our experimental conditions the reoxygenation phases reverted IRP modulation by OGSD. The re-establishment of IRPs activity by normoxic conditions agrees with reports on non-excitable cells (Tacchini *et al.*, 2002; Hanson and Leibold, 1998; Schneider and Leibold, 2003).

The results obtained during reoxygenation can be ascribed to restoration of oxygen level or to production of radical oxygen species (ROS) that elicit activation of IRP1 (Hanson and Leibold, 1998).

Next, we investigated the effects of hypoxia/reoxygenation on the expression of the main proteins involved in iron metabolism, ferritin and transferrin receptor (TfR). Regarding TfR, hypoxic conditions induced a reduction of its expression, while there was a significant increase during reoxygenation phases. Accordingly, OGSD led to a significant reduction of TfR mRNA levels, while there was an up-regulation during the reoxygenation. Interestingly, the reoxygenation-induced increase of TfR content was more evident after an hypoxic exposure of 6h. Both transcriptional and post-transcriptional mechanisms appeared to operate during OGSD and OGSD/reoxygenation

Concerning ferritin cellular content, it resulted unchanged after 3h of OGSD, while there was a significant enhanced expression during reoxygenation. Interestingly, the reoxygenation-induced increase of ferritin content was less evident after an hypoxic exposure of 6h.

The level of H-ferritin mRNA resulted unchanged after brief-term hypoxic conditions (3h) and following reoxygenation, thus suggesting the ferritin expression was regulated by the post-transcriptional mechanism operated by IRPs. In a different way, a prolonged OGSD exposure (6h) caused a reduction of H-ferritin mRNA and an increase during the reoxygenation phases. In long-term hypoxic conditions ferritin expression seemed to be dependent on a coupled transcriptional and post-transcriptional control.

As predicted, the cytoprotective role exerted by ferritin is principally appreciable during the reoxygenation phase, when the oxygen availability promotes the iron-induced ROS production. However, in our experimental conditions the defensive function of this protein is less manifest after long-term hypoxic conditions. In these conditions the diverse ferritin and TfR expression could explain the minor resistance of the cells to OGD/reoxygenation injury.

In conclusion, in our *in vitro* experimental model of ischemia the "point of no return" of the H9c2 cardiac cells, is fixed approximately at 6 hours of hypoxic conditions. After this point, increased misregulations of iron metabolism coupled to reduction of oxygen availability caused permanent damages and impaired cell survival.

REFERENCES

Abete, P., Napoli, C., Santoro, G., Ferrara, N., Tritto, I., Chiariello, M., Rengo, F., Ambrosio, G. (1999). Age-related decrease in cardiac tolerance to oxidative stress. ***J Mol Cell Cardiol.*** **1,** 227-36

Abete, P., Calabrese, C., Ferrara, N., Coppa, A., Pisanelli, P., Cacciatore, F., Longobardi, G., Napoli, C., Rengo, F. (2000). Exercise training restores ischemic preconditioning in the aging heart. ***J Am Coll Cardiol.*** **2,** 643-50

Abbound, S., Haile, D. J. (2000). A novel mammalian iron-regulated protein involved in intracellular iron metabolism. ***J. Biol. Chem***. **275**, 19906-19912

Allikmets, R., Raskind, W. H., Hutchinson, A., Schueck, N. D., Dean, M., Koeller, D. M., (1999). Mutation of a putative mitochondrial iron transporter gene (ABC7) in X-linked sideroblastic anemia and ataxia (XLSA/A). ***Hum. Mol. Genet***. **8**, 743-749

Andersen, O., Pantopoulos, K., Kao, H. T., Muckenthaler, M., Youson, J. H., Pieribone, V., (1998). Regulation of iron in the sanguivore lamprey *Lampetra fluviatilis*-molecular cloning of two ferritin subunits and two iron regulatory proteins (IRP) reveals evolutionary conservation of the iron-regulatory element (IRE)/IRP regulatory system. ***Eur. J. Biochem***. **254**, 223-229

Arteaga, C., Canet, E., Ovize, M., Janier, M., Revel, D. (1994). Myocardial perfusion assessed by subsecond magnetic resonance imaging with a paramagnetic macromolecular contrast agent. ***Invest Radiol.*** **4,** S54-7

Bemis, L., Chan, D. A., Finkielstein, C. V., Qi, L., Sutphin, P. D., Chen, X., Stenmark, K., Giaccia, A. J., Zundel, W., (2004). Distinct aerobic and hypoxic mechanisms of HIF-alpha regulation by CSN5. ***Genes Dev***. **18**, 739-744

Bothwell TH., (1995). Overview and mechanisms of iron regulation. ***Nutr. Rev***. **53,** 237-45

Bouton, C., Hirling, H., Drapier, J.C. (1997) Redox modulation of iron regulatory proteins by peroxynitrite. ***J. Biol. Chem***. **272**, 19969-19975

Brissot, P., Troadec, M.B., Loréal, O. (2004). The clinical relevance of new insights in iron transport and metabolism. ***Curr Hematol Rep.*** **2,** 107-15. Review

Broderick,T.L., Driedzic, W.R., Gillis, M., Jacob, J., Belke, T. (2001). Effects of chronic food restriction and exercise training on the recovery of cardiac function following ischemia. ***J Gerontol A Biol Sci Med Sci.*** **1,** B33-7

Cabantchik, Z.I., Glickstein, H., Milgram, P., Breuer, W., (1996). A fluorescence assay for assessing chelation of intracellular iron in a membrane model system and in mammalian cells. ***Anal Biochem.*** **2,** 221-7

Cairo, G, Pietrangelo, A., (2000). Iron regulatory proteins in pathobiology. ***Biochem J.*** **352**, 241-50

Cairo, G., Recalcati, S., Pietrangelo, A., Minotti, G., (2002). The iron regulatory proteins: targets and modulators of free radical reactions and oxidative damage. ***Free Radic. Biol.*** **32**, 1237-43

Cheepsunthorn, P., Palmer, C., Menzies, S., Roberts, R. L., Connor, J. R., (2001). Hypoxic/ischemic insult alters ferritin expression and myelination in neonatal rat brains. ***J. Comp. Neurol***. **431**, 382-396

Chi, S. I., Wang, C. K., Chen, J. J., Chau, L. Y., Lin, T. N., (2000). Differential regulation of H and L ferritin messenger RNA subunit, ferritin protein and iron following focal cerebral ischemia-reperfusion. ***Neuroscience*** **100**, 475-484

Chomczynski, P., Sacchi, N., (1987). Single-step method of RNA isolation by acid guanidinium thiocyanate-phenol-chloroform extraction. ***Anal Biochem***. **162**,156-159

Donovan, A., Brownlie, A., Zhou, Y., Shepard, J., Pratt, S. J., Moynihan, J., Paw, B. H., Drejer, A., Barut, B., Zapata, A., Law, T. C., Brugnara, C., Lux, S. E., Pinkus, G. S., Pinkus, J. L., Kingsley, P. D., Palis, J., Fleming, M. D., Andrews, N.C., Zon, L. I., (2000). Positional cloning of zebrafish ferroportin1 identifies a conserved vertebrate iron exporter. ***Nature.*** **403**, 776-781

Eisenstein, R. S., Blemings, K. P., (1998). Iron regulatory proteins, iron responsive elements and iron homeostasis. ***J. Nutr***. **128**, 2295-2298

Ema, M., Taya, S., Yokotan,i N., Sogawa, K., Matsuda, Y., Fujii-Kuriyama, Y. A novel bHLH-PAS factor with close sequence similarity to hypoxia-inducible factor 1alpha regulates the VEGF expression and is potentially involved in lung and vascular development***. Proc. Nat.l Acad. Sci.*** *USA*. 94, 4273-4278

Esterbauer, H., Cheeseman, K. H., (1990). Determination of aldehydic lipid peroxidation products: malonaldehyde and 4-hydroxynonenal. ***Methods Enzymol***. **186**,407-421

Ferriera, C., Bucchini, D., Martin, M. E., Levi S, Arosio P, Grandchamp B, Beaumont C. (2000). Early embryonic lethality of H ferritin gene deletion in mice. ***J. Biol. Chem***. **275**, 3021-3024

Festa, M., Colonna, A., Pietropaolo, C., Ruffo, A. (2000). Oxalomalate, a competitive inhibitor of aconitase, modulates the RNA-binding activity of iron-regulatory proteins. ***Biochem***. *J.* **348**, 315-320

Ganz T. (2003). Hepcidin, a key regulator of iron metabolism and mediator of anemia of inflammation. ***Blood***. 102:783-788

Gu, Y. Z., Moran, S. M., Hogenesch, J. B., Wartman, L., Bradfield, C. A., (1998) Molecular characterization and chromosomal localization of a third alpha-class hypoxia inducible factor subunit, HIF3alpha. ***Gene Expr***. **7**, 205-213

Gunshin, H., Mackenzie, B., Berger, U.V., Gunshin, Y., Romero, M.F., Boron, W.F., Nussberger, S., Gollan, J.L., Hediger, M.A. (1997). Cloning and characterization of a mammalian proton-coupled metal-ion transporter. ***Nature.*** **6641,** 482-8

Halliwell, B., Gutteridge, J.M. (1990). The role of free radicals and catalytic metal ions in human disease: an overview. ***Methods Enzymol.*** **186**, 1-85

Halliwell B., (1992). Reactive oxygen species and the central nervous system. ***J. Neurochem***. ***59***, 1609-1623

Hanson, E. S. Leibold, E. A., (1998). Regulation of iron regulatory protein 1 during hypoxia and hypoxia/reoxygenation. ***J. Biol. Chem***. **273**, 7588-7593

Hanson, E.S., Foot, L. M., Leibold, E. A. (1999). Hypoxia post-translationally activates iron-regulatory protein 2. ***J. Biol. Chem***. **274**, 5047-5052

Hara, S., Hamada, J., Kobayashi, C., Kondo, Y., Imura, N., (2001). Expression and characterization of hypoxia-inducible factor (HIF)-3alpha in human kidney: suppression of HIF-mediated gene expression by HIF-3alpha. ***Biochem. Biophys Re. Commun.*** **287**, 808-813

Harrison, P.M., Arosio, P. (1996). The ferritins: molecular properties, iron storage function and cellular regulation. ***Biochim. Biophys. Acta*** **1275**, 161-203

Hogenesch, J. B., Chan, W. K., Jackiw, V. H., Brown, R. C., Gu, Y. Z., Pray-Grant, M., Perdew, G. H., Bradfield, C. A., (1997). Characterization of a subset of the basic-helix-loop-helix-PAS superfamily that interacts with components of the dioxin signaling pathway. ***J. Biol. Chem***. **272**, 8581-8593

Huang, L. E., Gu, J., Schau, M., Bunn, H. F., (1998). Regulation of hypoxia-inducible factor 1α is mediated by an oxygen dependent domain via the ubiquitin –proteosome pathway. ***Proc. Natl. Acad. Sci.*** *USA* **95**, 7987-7992

Hutter, M.M., Sievers, R.E., Barbosa, V., Wolfe, C.L. (1994). Heat-shock protein induction in rat hearts. A direct correlation between the amount of heat-shock protein induced and the degree of myocardial protection. ***Circulation.*** **89**, 355-60

Irace C, Scorziello A, Maffettone C, Pignataro G, Matrone C, Adornetto A, Santamaria R, Annunziato L, Colonna A. (2005) Divergent modulation of iron regulatory proteins and ferritin biosynthesis by hypoxia/reoxygenation in neurones and glial cells. ***Journal of Neurochemistry***, **95**, 1321-1331

Ischiropoulos, H., Beckman, J. S., (2003). Oxidative stress and nitration in neurodegeneration: cause, effect, or association? ***J. Clin. Invest.*** **111**, 163-169

Iwai, K., Drake, S. K., Wehr, N. B., Weissman, A. M., LaVaute, T., Minato, N., Klausner, R. D., Levine, R. L., Rouault, T. A., (1998). Iron-dependent oxidation, ubiquitination, and degradation of iron regulatory protein 2: implications for degradation of oxidized proteins. ***Proc Natl Acad Sci*** *USA*. **95**, 4924-4928

Kakhlon, O., Gruenbaum, Y., Cabantchik, Z. l., (2001). Repression of the heavy ferritin chain increases the labile iron pool of human K562 cells. ***Biochem. J.*****, 356**, 311-316

Knight, S. A. B., Babu, N., Sepuri, V., Pain, D., Dancis, A. (1998). Mt-Hsp70 homolog, Ssc2p, required for maturation of yeast frataxin and mitochondrial iron homeostasis. ***J. Biol. Chem***. **273**, 18839-18893

Kondo, T., Shirasawa, T., Itoyama,Y., Mori, H., (1996) Embryonic genes expressed in Alzheimer's disease brains. *Neurosci Lett.* **209**, 157-160

Konijn, A. M., Glickstein, H., Vaisman, B., Meyron-Holtz, E. G., Slotki, I. N., Cabantchik, Z. I. (1999). The cellular labile iron pool and intracellular ferritin in K562 cell. ***Blood*** **94**, 2128-2134

Kuriyama-Matsumura, K., Sato, H., Suzuki, M., Banai, S., (2001). Effects of hyperoxia and iron on iron regulatory protein-1 activity and ferritin synthesis in mouse peritoneal macrophages. *Biochim.* ***Biophys Acta* Protein Struct. Mol . *Enzymol***. **1544**, 370-377

Lakatta, E.G., Sollott, S.J. (2002). Perspectives on mammalian cardiovascular aging: humans to molecules. ***Comp Biochem Physiol A Mol Integr Physiol*.4,** 699-721 Review.

Lange, H., Kispal, G., Lill, R. (1999). Mechanism of iron transport to the site of heme synthesis inside yeast mitochondria. ***J. Biol. Chem***. **274**, 18989-18996

LaVaute, T., Smith, S., Cooperman, S., Iwai, K., Land, W., Meyron-Holtz, Drake, S. K., Miller, G., Abu-Asab, M., Tsokos, M., Switzer III, R., Grinberg, A., Love, P., Tresser, N., Rouault, T. A., (2001). Targeted deletion of the gene encoding iron regulatory protein-2 causes misregulation of iron metabolism and neurodegenerative disease in mice. ***Nat. Genet.* 27**, 209-214

LeBel, C.P., Ischiropoulos, H., Bondy, S.C., (1992). Evaluation of the probe 2',7'-dichlorofluorescin as an indicator of reactive oxygen species formation and oxidative stress. ***Chem Res Toxicol.* 2,** 227-31.

Levi, S., Corsi, B., Bosisio, M., Invernizzi, R., Volz, A., Sanford, D., Arosio, P., Drysdale, J., (2001). A human mitochondrial ferritin encoded by an intronless gene. ***J Biol Chem***. **276**, 24437-24440

Linert, W., Jameson, G. N., (2000) Redox reactions of neurotransmitters possibly involved in the progression of Parkinson's Disease. *J. Inorg. Biochem*. **79**, 319-26

Locke, M., Tanguay, R.M., Klabunde, R.E., Ianuzzo, C.D. (1995). Enhanced postischemic myocardial recovery following exercise induction of HSP 72. ***Am J Physiol.* 269(1 Pt 2),** H320-5.

Mariani, J., Ou, R., Bailey, M., Rowland, M., Nagley, P., Rosenfeldt, F., Pepe, S. (2000). Tolerance to ischemia and hypoxia is reduced in aged human myocardium. ***J Thorac Cardiovasc Surg.* 4,** 660-7.

Maxwell, P. H., Wiesener, M. S., Chang, G. W., Clifford, S. C., Vaux, E. C., Cockaman, M. E., Wykoff, C. C., Pugh, C. W., Maher, E. R., Ratcliffe, P. J.,

(1999). The tumor suppressor protein VHL targets hypoxia-inducible factors for oxygen-dependent proteolysis. ***Nature* 399**, 271-275

McKie, A. T., Marciani, P., Rolfs, A., Brennan, K., Wehr, K., Barrow, D., Miret, S., Bomford, A., Peters, T. J., Farzaneh, F., Hediger, M. A., Hentze, M. W., Simpson, R. J., (2000). A novel duodenal iron-regulated transporter, IREG1, implicated in the basolateral transfer of iron to the circulation. ***Mol. Cell***. **5**, 299-309

McKie, A. T., Barrow, D., Latunde-Dada, G. O., Rolfs, A., Sager, G., Mudaly, E., Mudaly, l., Richardson, C., Barlow, D., Bomford, A., Peters, T. J., Raja, K. B., Shirali, S., Hediger, M. A., Farzaneh, F., Simpson, R. J., (2001). An iron-regulated ferric reductase associated with the absorption of dietary iron. ***Science* 291**, 1755-1759

Meyron-Holtz E. G., Ghosh M. C. and Rouault T. A. (2004) Mammalian tissue oxygen levels modulate iron-regulatory protein activities in vivo. ***Science* 306**, 2087–2090

Neilands, JB. (1991). A brief history of iron metabolism. ***Biol. Met*** . **4**, 1-6

Nemeth, E., Tuttle, M.S., Powelson, J., Vaughn, M.B., Donovan, A., Ward, D.M., Ganz, T., Kaplan, J. (2004). Hepcidin regulates cellular iron efflux by binding to ferroportin and inducing its internalization. ***Science.* 5704,** 2090-3

Opie, L.H. (1998). Review of trials in the treatment of coronary artery disease: theoretical expectations versus lack of practical success--how can we explain the differences? ***Am J Cardiol.* 3A,** 15H-20H.

Piper, H. M., Abdallah, Y. and Schaefer, C. (2004) The first minutes of reperfusion: a window of opportunity for cardioprotection. ***Cardiovasc. Res.* 61**, 365–371

Ponka, P., Beaumont, C., Richardson, D. R., (1998). Function and regulation of transferrin and ferritin. ***Semin. Hematol***. **35**, 35-54

Ponka, P. (1997). Tissue-specific regulation of iron metabolism and heme synthesis: distinct control mechanisms in erythroid cells. ***Blood* 90**, 473-474

Prus, E., Fibach, E. (2008). The labile iron pool in human erythroid cells. ***Br J Haematol.*** May 22. [Epub ahead of print]

Qi, Y., Jamindar, T. M., Dawson, G., (1995). Hypoxia alters iron homeostasis and induces ferritin synthesis in oligodendrocytes. ***J. Neurochem***. **64**, 2458-2464

Rolfs, A., Kvietikova, I., Gassmann, M., Wenger, R. H., (1997). Oxygen-regulated transferrin expression is mediated by hypoxia-inducible factor 1. ***J. Biol. Chem***. **272**, 20055-20062

Rucker, P., Torti, F. M., Torti, S. V., (1996). Role of H and L subunits in muose ferritin. ***J. Biol. Chem***. **271**, 33352-33357

Ryter, S.W, Tyrrell, R.M. (2000). The heme synthesis and degradation pathways: role in oxidant sensitivity. Heme oxygenase has both pro- and antioxidant properties. ***Free Radic Biol Med.*** **2,** 289-309. Review

Schneider, B.D., Leibold, E.A. (2003) Effects of iron regulatory protein regulation on iron homeostasis during hypoxia. ***Blood*** **102**, 3404-3411

Schulman, D., Latchman, D.S., Yellon, D.M. (2001). Effect of aging on the ability of preconditioning to protect rat hearts from ischemia-reperfusion injury. ***Am J Physiol Heart Circ Physiol.*** **4,** H1630-6

Semenza, G. L., Agani, F., Booth, G., Forsythe, J., Iyer, N., Jiang, B. H., Leung, S., Roe, R., Wiener, C., Yu, A., (1997). Structural and functional analysis of hypoxia-inducible factor 1. ***Kidney Int.*** **51**, 553-555

Sharma, A., Singh, M.(2001). Protein kinase C activation and cardioprotective effect of preconditioning with oxidative stress in isolated rat heart. ***Mol Cell Biochem.*** **1-2,** 1-6

Sipe, D. M., Murphy, R. F., (1991). Binding to cellular receptors results in increased iron release from transferrin at mildly acidic pH. ***J. Biol. Chem.*** **266**, 8002-8007

Solaini, G. and Harris, D.A., (2005). Biochemical dysfunction in heart mitochondria exposed to ischaemia and reperfusion. ***Biochem. J.*** **390**, 377-394

Soum, E., Brazzolotto, X., Goussias, C., Bouton, C., Moulis, J. M., Mattioli, T. A., Drapier, J. C., (2003). Peroxynitrite and nitric oxide differently target the iron-sulfur cluster and amino acid residues of human iron regulatory protein 1. ***Biochemistry.*** **42**, 7648-7254

Starnes, J.W., Bowles, D.K., Seiler. K.S. (1997). Myocardial injury after hypoxia in immature, adult and aged rats. ***Aging.*** **4,** 268-76.

Tacchini, L., Recalcati, S., Bernelli-Zazzara, A., Cairo, G., (1997). Induction of ferritin synthesis in ischemic-reperfused rat liver: analysis of the molecular mechanisms. ***Gastroenterology***. **113,** 946-953

Tacchini, L., Bianchi, L., Bernelli-Zazzera, A., Cario, G., (1999). Transferrin receptor induction by hypoxia. ***J. Biol. Chem***. **274**, 24142-24146

Tacchini, L., Fusar Poli, D., Bernelli-Zazzera, A., Cairo, G., (2002) Transferrin receptor gene expression and transferrin-bound iron uptake are increased during postischemic rat liver reperfusion. *Hepatology* **36**, 103-111

Tian, H., McKnight, S. L., Russell, D. W., (1997). Endothelial PAS domain protein 1 (EPAS1), a transcription factor selectively expressed in endothelial cells. *Genes Dev*. **11,** 72-82

Torti, F.M., Torti, S.V. (2002). Regulation of ferritin genes and protein. ***Blood.*** **10,** 993505-16. Review

Toth, I., Yuan, L. P., Rogers, J. T., Boyce, H., Bridges, K. R., (1999). Hypoxia alters iron-regulatory protein-1 binding capacity and modulates cellular iron homeostasis in human hepatoma and erythroleukemia cells. ***J. Biol. Chem***. **274**, 4467-4473

Vulpe ,C. D., Kuo, Y. M., Murphy, T. L., Cowley, L., Askwith, C., Libina, N., Gitschier, J., Anderson, G. J., (1999). Hephaestin, a ceruloplasmin homologue implicated in intestinal iron transport, is defective in the sla mouse. ***Nat Genet***. **21,** 195-199

Wallander, M.L, Leibold, E.A, Eisenstein, R.S. (2006). Molecular control of vertebrate iron homeostasis by iron regulatory proteins. ***Biochim Biophys Acta.*** **17,** 668-89 Review

.

Wenger, R. H., (2002). Cellular adaptation to hypoxia: O2-sensing protein hydroxylases, hypoxia-inducible transcription factors, and O2-regulated gene expression. *FASEB J*. **16**, 1151-1162

Wiesener, M. S., Turley, H., Allen, W. E., Willam, C., Eckardt, K. U., Talks, K. L., Wood, S. M., Gatter, K. C., Harris, A. L., Pugh, C. W., Ratcliffe, P. J., Maxwell, P. H., (1998). Induction of endothelial PAS domain protein-1 by

hypoxia: characterization and comparison with hypoxia-inducible factor-1alpha. ***Blood*** **92**, 2260-2268

Wood R.J., Ronnenberg A.G., Iron, 10th ed., Lippincott Williams and Wilkins, Philadelphia, PA, 2006.

Yu, J., Wessling-Resnick, M. (1998). Structural and functional analysis of SFT, a stimulator of Fe Transport. ***J Biol Chem.*** **33,** 21380-5